OPTIMIZATION OF BRIDGE FORMS

A DISSERTATION

Submitted in partial fulfilment of the

requirements for the award of the degree

of

MASTER OF TECHNOLOGY

in

CIVIL ENGINEERING

(With Specialization in Structural Engineering)

By

ANURAG ANAND

(17523006)

DEPARTMENT OF CIVIL ENGINEERING

INDIAN INSTITUTE OF TECHNOLOGY ROORKEE

ROORKEE – 247 667 (INDIA)

MAY, 2019

CANDIDATE'S DECLARATION

I hereby certify that the work which is being presented in this Dissertation Report titled **"OPTIMIZATION OF BRIDGE FORMS"** in the partial fulfillment of the requirement for the award of degree of Master of Technology has been by carried out by me in the Department of Civil Engineering, Indian Institute of Technology Roorkee, under the supervision of Professor **Dr. Vipul Prakash**.

The matter presented in this report has not been submitted by me for the award of any other degree in this or any other institute.

Date:
Place: Roorkee

[ANURAG ANAND]
Enrolment No. 17523006

CERTIFICATE

This is to certify that **Anurag Anand**, Enrolment Number – 17523006, pursuing M.Tech. in Structural Engineering, IIT Roorkee, has worked under my supervision on the dissertation titled '**Optimization of Bridge Forms'**, which has been completed in May, 2019. The declaration made by the candidate is true to the best of my knowledge and beliefs.

Date:
Place: Roorkee

[Dr. VIPUL PRAKASH]
Professor,
Department of Civil Engineering,
Indian Institute of Technology, Roorkee.

ACKNOWLEDGEMENTS

At the outset, I would like to acknowledge the role of my dissertation mentor, Dr. Vipul Prakash, without whose guidance this work would have been impossible. His emphasis on fundamentals of the subject helped develop deeper conceptual insights, and his self was an invigorating inspiration when progress used to be difficult. I also acknowledge Arya Prakash Padhi for his untiring help with Abaqus; without his help the progress of this work would have been unimaginably impaired. Dr. Anupam Chakrabarti is thankfully acknowledged for being kind enough to allow to use his resources when it was necessary.

As ever, unspoken words of gratitude shall always remain for my friends, family and the Almighty, who have always been there as a bolster to life in general.

List of Figures		
Figure no.	**Description**	**Page No.**
2.1	Different regions satisfying Michell's optimality criteria	5
2.2	Michell forms for: (a) cantilever loaded at the tip and supported at two points; (b) optimal support structure for a centrally loaded simply supported beam; (c) half of a middle-loaded beam	5
2.3	Mitchell's half-wheel for transmitting a uniformly distributed load to a centrally pinned line segment	6
2.4	Parameter X being used to divide the domain into regions for adhering to kinematic admissibility	6
2.5	Different structural forms obtained by varying the ratios of limiting compressive to tensile strengths	7
2.6	Fig 2.6: (a) Ground structure; (b) exact optimal layout; approximate discretized solutions from (c) – (e)	8
2.7	Optimized bridge forms obtained for spans of 1km, 2.5 km and 5 km, respectively, exhibiting hybrid Michell half-wheel forms	10
2.8	A simple truss used to show the procedure of drawing force diagrams	14
4.1	Design domain with dimensions (mm), loading type and boundary conditions. Model corresponds to a rise : span of 0.4	18
4.2	Design space for long span bridge with dimensions (m), loading type and boundary conditions	19
4.3	Dimensions of the design space in Rhino 3D	20
4.4	Grasshopper canvas with parameters assigned to components that are arranged in a circuital flow chart	21
5.1	Effect on strain energy by changing rise to span ratios for various volume fractions.	22
5.2	Two forms, corresponding to volume fraction of 0.1 for a rise : span of (a) 0.1; (b) 0.2	23
5.3	Three forms, corresponding to rise : span of 0.1, for volume fraction (a) 0.1; (b) 0.3; (c) 0.5	24
5.4	Variation of strain energy with rise : span for a constant volume	24

CONTENTS

CHAPTER 1 - INTRODUCTION

One of the most fundamental parameters that determine the efficiency of a structural design is the *form* of the structure. Absence of the best geometry, interconnectivity, and disposition of the members to resist the loads, is crippling to any improvement that can be otherwise made in the structural design. The ideal form to carry the imposed loads enables the most economical design, in the sense that material weight, or volume, is minimum, as the size of every member is just enough to develop the allowable stress, and the process of finding the ideal form leads to, and remarkably, is also led by, clarity and deeper insights into the behavior of the structure. Emphasis had been paid on the importance of the ideal form since the time of Maxwell and Cremona, who harnessed the lucidity of geometry to study the problems of static equilibrium, through which developed the tools that helped the structural engineers in the coming times to build a variety of bridges, domes and towers – all without the help of computers. With the availability of immense computational resources at present, the problem of finding the *optimum* structural parameters for design – like, stiffness, weight or volume – has began to gain attention steadily.

In case of bridges, the suitability of form assumes an ever-important role because the correct form makes the structure lighter, more economical, and stiffer, i.e. the resulting deflections are also less. Also, in case of long span bridges, the dead load of the structure is the dominant load which the bridge form has to carry, so reducing the weight of the structure also means that longer spans can be achieved. For this, one could go for the choice of lighter materials like carbon fiber composites. However, the problem of ductility, fatigue behavior, relative cost and availability of materials suggests that steel and concrete are going to be the dominant materials for construction for a good time to come. Hence, the most relevant parameter that remains at hand for optimizing the weight of the structure is the structural form.

The results that follow the optimization of the *layout* of the structure are often counterintuitive. For example, common knowledge prevailed that a parabolic arch is the most optimum form to distribute a uniformly distributed load between two hinged supports. However, layout optimization has showed that it is not the case – rather, the most efficient form consists of a

parabolic section near the central part of the span, and a network of mutually perpendicular compressive and tensile elements near the supports – a form of structure which came to be known as Hemp's arch[1]. Hence, a reasonable question rises to the fore: are the traditional bridge forms the most efficient for bearing the loads they are principally subjected to? In case of arch bridges, is the conventional form with arch supplemented with vertical suspenders the most efficient? Is there a better form to carry the loads for longer spans than the conventional cable stayed and suspension bridge systems? If yes, how can those bridge forms be obtained? What structural parameters should be optimized, and what should be the proper choice of constraints? Finally, once the optimized bridge forms are obtained, can these forms be rationalized through the fundamental aspects of structural mechanics instead of relying on mathematical or numerical results alone?

In this study, we address the structural optimization problem in context to the structures and loadings that correspond to that of typical bridge systems. We discuss the different approaches towards the choice of the objective that determines the optimization problem, and explore them to see if they provide with the same solution in regards to the resulting forms. It will be observed that most of the weight minimization problems employ stresses as constraints. Furthermore, they are mostly based on the *ground structure approach* as shall be seen. Will the same form remain optimal for *compliance minimization* as an objective, over a continuous domain? We shall examine these aspects of the bridge forms developed from the compliance minimization problem. Thereafter, we review those forms in the light of fundamental aspects of statics to get a deeper insight into their behavior, so as to get a rationale if they indeed, from the standpoint of statics alone and not computation, show the features of the most ideal form which is required of them by statics.

In order to minimize compliance, the formulation conventionally used, which will be used here, minimizes strain energy – naturally, more is the flexibility or compliance, more is the strain energy. A minimum compliance or strain energy structure is also a maximum stiffness structure. Hence, in reference to the optimization objective, *minimizing strain energy* or *compliance* and *maximizing stiffness* refer to the same goal.

CHAPTER 2 – LITERATURE REVIEW

2.1 Layout Optimization

2.1.1 Components of the Optimization Problem

The layout of structure is said to be optimum when the following features of the structures are optimized simultaneously:

- The *topology* of the structure, i.e. the mutual arrangement of the different members and joints in the design domain.
- *Geometry* of the structure, i.e. the overall outline of the structural form which is governed by the position of the joints.
- *Size*, or the cross-sectional dimensions of the various structural members.

Usually, the goal of the optimization is formulated in the form of an *objective function* which is sought to be minimized, with suitable constraints. The objective function may be the weight, volume or the compliance of the structure, and the constraints may be the geometry of the structure (any prescribed minimum size of the members), final volume of the structure (or, the minimum volume from the design domain that must be retained in the final structure), or one of the structural behaviors such as stresses and displacements. The choice of objective functions and constraints are concomitant, and as will further be outlined, such choices result in two major approaches towards structural optimization: one that deals with minimizing the compliance with a weight (volume) constraint, and the other that deals with minimizing the weight (volume) with stress constraints.

Broadly, there are two approaches to solve the optimization problem for a given structure: *exact* formulation which is an analytical method that gives exact and closed-form solutions, and the *approximate* formulation, which depends on the discretization of the design domain or the material properties to obtain iterative, numerical solutions. While exact formulations have been used to establish the ground work in the discipline of structural optimization, it is the approximate formulations that are mostly used for more complex structures to harness the benefit of computational power.

2.1.2 Exact Formulation[21]

The theory of exact optimal layout involves the following concepts:

- *Design Domain*: It is superset of configurations of which the optimal structure is a subset. Also known as structure universe, it comprises of members running in all possible directions, present at all available points in the space.
- *Continuum type Optimality Criteria*: The optimality criteria are the necessary and often sufficient conditions for optimization. They can be seen as a mechanical interpretation of Kahn-Tucker conditions that mathematically govern the optimality of the solution to an optimization problem.
- *Adjoint Structure*: It is fictitious structure to exhibit the mechanical analogy to interpret certain aspects of the optimality criteria.
- *Layout Criterion Function*: The optimality criteria are used to derive the layout criterion function φ^e, which decides in which directions shall the members be oriented by taking such a form where

  $$\varphi^e = 1 \text{ (for } A^e \neq 0); \ \varphi^e \leq 1 \text{ (for } A^e = 0),$$

  where A^e is the cross section of the member '*e*'.

Both the real and adjoint strain fields are defined at every point in the design domain, and should both be kinematically admissible for both the boundary conditions at the supports and compatibility conditions in the interior of the design domain. The layout criterion function should assume a unit value in at least one direction at every point of the design domain, and members should be laid out only in these directions, such that the resulting structure can be stable to transmit the loads.

Exact formulation reveals the basic structural essence of the optimal systems. In the least, they are important because they serve as standard yardsticks around which the validity, global optimality and convergence of solutions based on numerical methods are evaluated. In case of the presence of more than one optimal form, analytical approach reveals all such forms, while a program based on a numerical approach, usually is random in selecting one of such forms.

❖ *Michell's Optimality Criteria*[2]

A. G. M. Michelle in his seminal work showed that for a structure with member having equal limiting stresses in both tension and compression to have minimum weight, every member should be aligned in the direction of principal strains. Solutions obtained, hence, consist of members running in mutually perpendicular directions, with each developing the prescribed limiting stress, either in tension or in compression. The resulting displacement field should also be consistent with the required kinematic and compatibility conditions.

Michell's Optimality Criteria can be satisfied in the following number of ways, implying that a domain containing an optimal structure consists of one or more of the following regions, defined by the member forces and corresponding principal strains, such as

R^+ : $f_1 > 0,\ f_2 = 0,\ \varepsilon_1 = 1,\ |\varepsilon_2| \leq 1$

R^- : $f_1 < 0,\ f_2 = 0,\ \varepsilon_1 = -1,\ |\varepsilon_2| \leq 1$

S^+: $f_1 > 0,\ f_2 > 0,\ \varepsilon_1 = 1,\ \varepsilon_2 = 1$

S^-: $f_1 < 0,\ f_2 < 0,\ \varepsilon_1 = -1,\ \varepsilon_2 = -1$

T: $f_1 > 0,\ f_2 < 0,\ \varepsilon_1 = 1,\ \varepsilon_2 = -1$

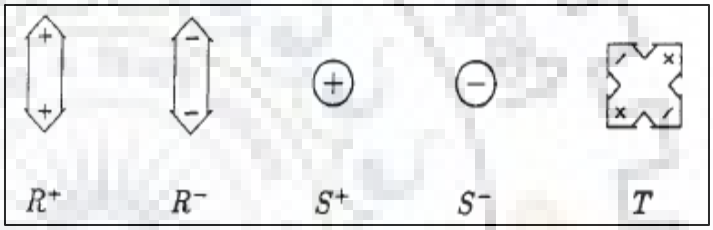

Fig 2.1: *Different regions satisfying Michell's optimality criteria (Rozvany et al., 1995)*

These criteria have been applied to many cases of loads and boundary conditions get a number of structural forms, some of which are shown in Fig 2.2.

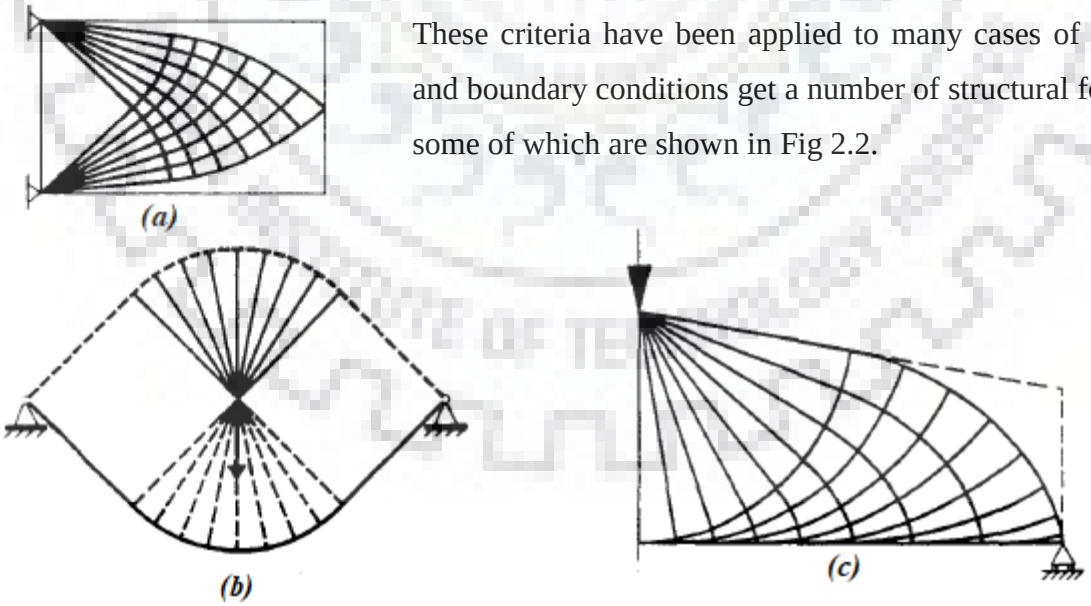

Fig 2.2: *Michell forms for: (a) cantilever loaded at the tip and supported at two points; (b) optimal support structure for a centrally loaded simply supported beam; (c) half of a middle-loaded beam (Rozvany et al.,1995)*

❖ *Bridge Forms identified using Michell's Criteria*[3]

The problem of an infinite line supported by pins at equal intervals, and loaded by a uniformly distributed load was considered by Pichugin et al[3]. The considered domain was a double segment of length *2L* supported at the center with the prescribed loading, and the resulting structure was a Michell's half wheel as shown in Fig 2.3.

Furthermore, the design domain was divided into two different kinds of optimal regions, T and R^+ as indicated in Fig 2.4. The indicated parameter X showing the line of transition of domains, determines the geometry of the structure. Such form of Michell structures were shown to be more optimum in weight than the original half wheel Michell structure.

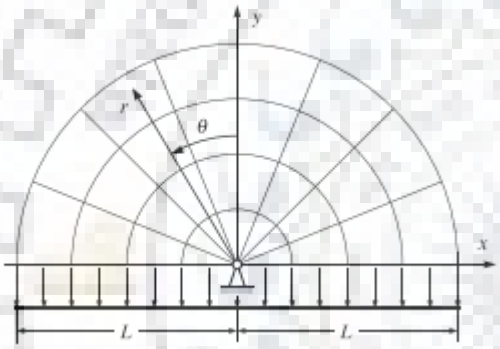

Fig 2.3: *Mitchell's half-wheel for transmitting a uniformly distributed load to a centrally pinned line segment. (Pichugin et al.,2015)*

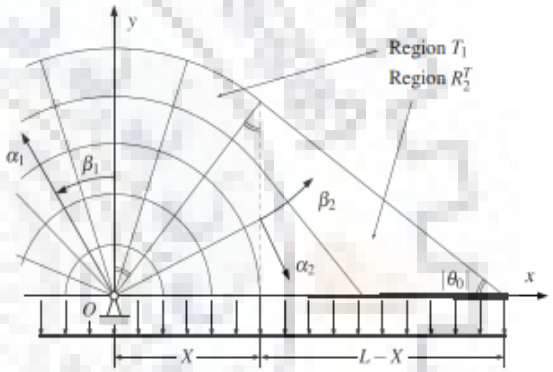

Fig 2.4: *Parameter X being used to divide the domain into regions for adhering to kinematic admissibility. (Pichugin et al.,2015)*

The parameter *X* is determined to be $X = \sigma_C.L/(\sigma_C + \sigma_T)$. Upon varying the ratio of the limiting compressive to tensile stresses, a family of bridge forms is obtained as shown in Fig 2.5. On making the design tension dominant, the spokes coalesce together near the vertical and the form is very similar to that of a cable stayed bridge, on the other hand, if the design is compression dominant, the fans shrink in size and the form resembles that of a Hemp's arch with vertical suspenders.

Thus, it was shown that cable stayed bridges and arch bridges lie at the opposite boundaries of the family of optimum bridge forms.

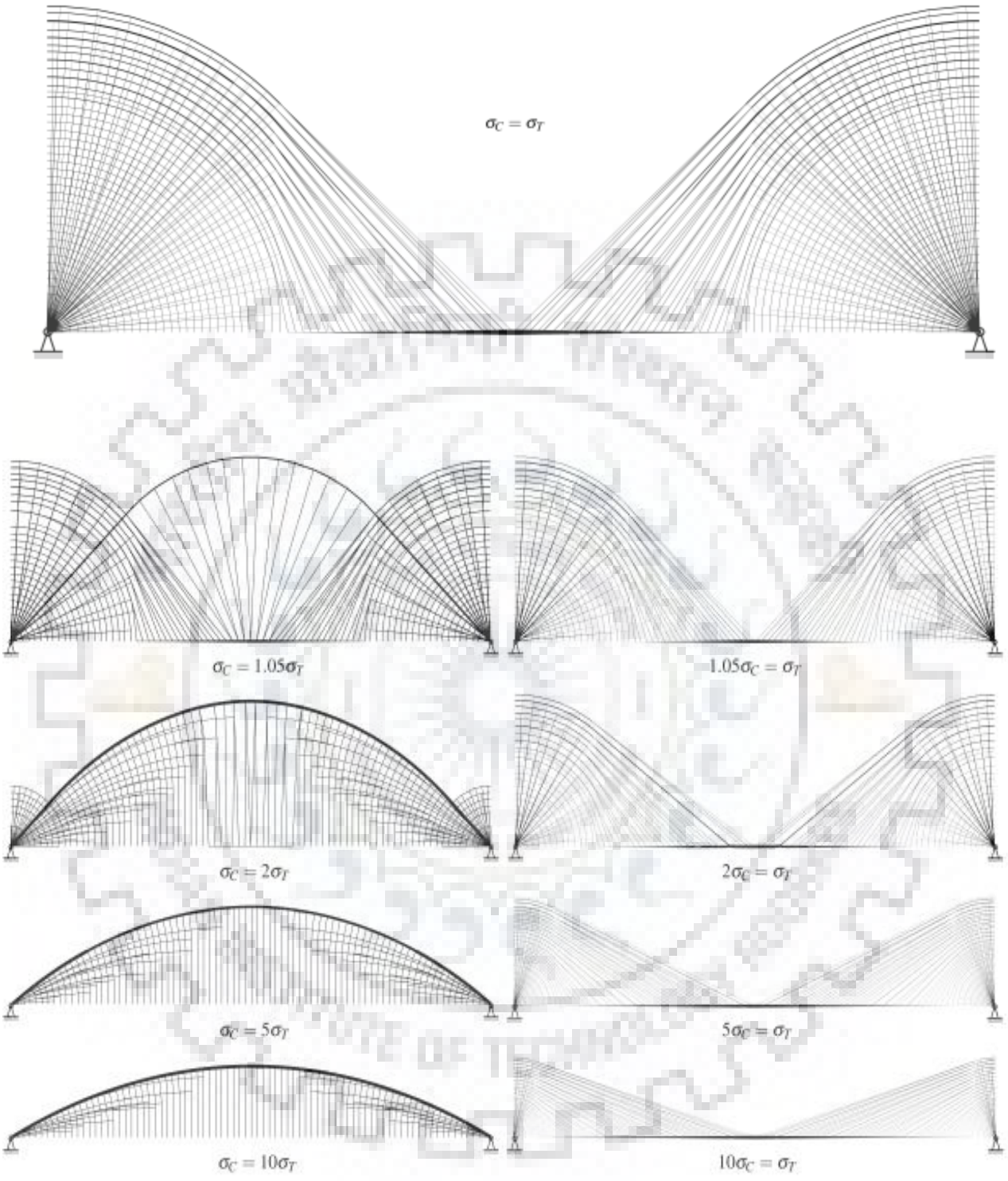

Fig 2.5: *Different structural forms obtained by varying the ratios of limiting compressive to tensile strengths. (Pichugin et al.,2015)*

2.1.3 Approximate Formulation

Exact analysis suffers from a handicap that it is applicable almost exclusively to certain ideal structural conditions; closed form solutions are very difficult to obtain for complicated geometry and loading. Apart from that, the solutions may be too complicated in geometry to be practical. That is where the emphasis is taken over by the approximate formulations, results from which have shown that even if a 'simplified' structure is considered, which has some finite number of members formed by joining with straight lines a finite number of joints from the optimal structure, it is still close to the optimal values in weight.

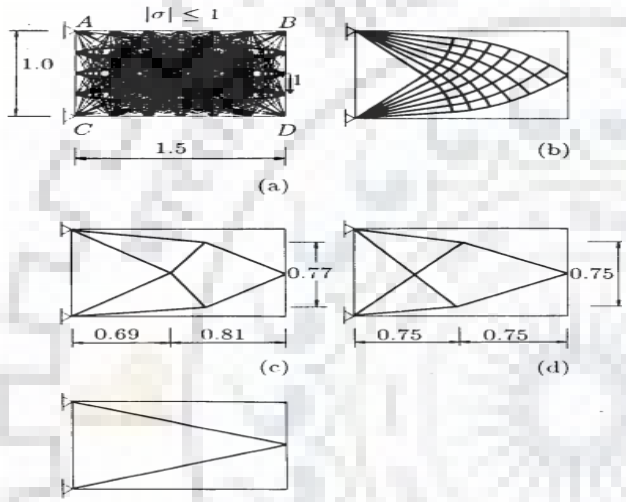

Fig 2.6: *(a) Ground structure; (b) exact optimal layout; approximate discretized solutions from (c) – (e) (Rozvany et al., 1995)*

Rozvany et. al have demonstrated this through an example shown in Fig 2.6. The exact optimal layout has a weight of 4.5, while the approximate discretized solutions shown in (c), (d) and (e) have weights 4.59, 4.69 and 5, respectively, showing that the discretized layouts are only insignificantly heavier than the exact layout[2].

In approximate formulation, the ground structure is constructed by considering a finite number of points in a domain of desired size and boundary conditions, and linking them together in all combinations with straight members. The *design variable* for the problem may be the cross-sectional areas of the members, or the position of joints. The objective function is to minimize the weight or volume, and constraints may be placed upon the stress levels in the members.

If both the objective function and constraints are a *linear* function of the design variable, then the problem can be solved using linear programming methods. In addition to it, if the feasible set is *convex*, then it is ensured that a local minimum obtained is also a global one.

To make the problem more amenable to automated solution, the structure is simplified, like, for example, only pin joints are considered, which makes the structure only axially loaded and as a matter of fact, also more optimum a-priori.

❖ *Linear Programming Formulation*[2]

The objective function to be minimized is the volume (in other words, weight) of the structure. If $\boldsymbol{L}$ is the member length vector and $\boldsymbol{X}$ is the variable set of cross sectional areas, then volume is given by

$$V = \boldsymbol{L}^T\boldsymbol{X}$$

The redundant forces $\boldsymbol{R}$ are provided by the compatibility equation,.

$$\boldsymbol{DR} = \boldsymbol{\delta}$$

where, $\boldsymbol{D}$ is the flexibility matrix, $\boldsymbol{\delta}$ the displacement vector in the direction of $\boldsymbol{R}$ due to the loading on the primary structure.

The forces $\boldsymbol{F}$ and the displacements $\boldsymbol{U}$ are given explicitly in terms of $\boldsymbol{X}$, $\boldsymbol{R}$ by

$$\boldsymbol{F} = \boldsymbol{F_P} + \boldsymbol{F_R}\boldsymbol{R},$$

$$\boldsymbol{U} = \boldsymbol{U_P} + \boldsymbol{U_R}\boldsymbol{R}$$

where, $\boldsymbol{F_P}$, $\boldsymbol{U_P}$ are vectors of forces and displacements respectively due to the loading on the primary structure, and $\boldsymbol{F_R}$, $\boldsymbol{U_R}$ are matrices of forces and displacements, respectively due to unit redundant forces in the primary structure. $\boldsymbol{F_P}$ and $\boldsymbol{F_R}$ are independent of the cross section, hence they don't change during the iterations.

Constraints are placed on the member forces by placing a bound on the permissible stresses ($\boldsymbol{\sigma_d}^L$, $\boldsymbol{\sigma_d}^U$). Displacements may also be used as constraints by placing a lower and upper bound ($\boldsymbol{U}^L$, $\boldsymbol{U}^U$) on them, such that:

$$\boldsymbol{\sigma_d}^L.\boldsymbol{X} \leq \boldsymbol{F} \leq \boldsymbol{\sigma_d}^U.\boldsymbol{X}$$

$$\boldsymbol{U}^L \leq \boldsymbol{U} \leq \boldsymbol{U}^U$$

And, if the load vector is given by $\boldsymbol{P}$ and the matrix of direction cosines by $\boldsymbol{B}$, equilibrium condition can be enforced by

$$\boldsymbol{BF} = \boldsymbol{P}$$

❖ *Optimum Bridge Forms by Ground Structure Approach*

Gilbert et al[4]. used an equivalent layout scheme based on the (plastic) lower bound theorem with the member forces ***q*** as the design variables, with an objective of minimizing the volume (weight) with two constraints: the system should be in equilibrium, the members should develop permissible stresses (equal in tension and compression everywhere).

Elements of catenaries of equal strength were used to link the nodes in the structural domain (Fig -. It was found that, when steel on density 80 kN/m^3 was used with a limiting stress of 500 MPa, spans up to 5 km could be achieved, and the bridge form was same as that of hybrid Michell half-wheel with two optimality regions (Fig 2.7). These bridges were lighter than other conventional forms for the same span, for example, as much as 73% lighter than a suspension bridge[4].

It is noteworthy that while the stresses developed and weight of the structure will definitely vary as the span is changed, the ideal form remains the same. It also adds to the insight developed from the exact analysis, that form is dependent on the loading and boundary conditions alone, not the spans involved.

It should also be noted that the objective function so far, has been the minimization of volume. All these structures have been obtained as a result of volume minimization, subject to stress constraints. Compliance as an objective function has not been incorporated into optimization studies with the ground structure approach.

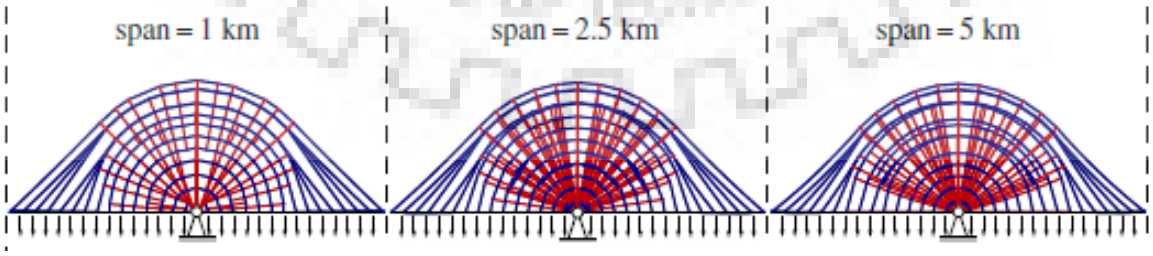

Fig 2.7: Optimized bridge forms obtained for spans of 1km, 2.5 km and 5 km, respectively, exhibiting hybrid Michell half-wheel forms. (Gilbert et al., 2018)

❖ *Solid Isotropic Material with Penalization (SIMP) Approach*

Instead of a discrete design domain consisting of a finite number of joints linked with a finite number of members, the design domain can also be chosen to be a continuum of material. The optimization can be performed on this domain using a variety of methods that are available today, the foremost of which is the SIMP approach.

In this approach, the density of the material is taken as the design variable. The goal of the optimization is usually to find the minimum compliance of the structure, subject to conditions of equilibrium volume available (as a fraction of the total volume of the design domain, typically). Often the objective is also formulated as strain energy instead of compliance for structures with complicated loadings, because of the knowledge that a minimum compliance results in maximum stiffness, and hence also the minimum strain energy.

The optimization procedure works by distributing the material in the design domain in such a way that the objective function (compliance or strain energy) is minimized. By default, an entire range of densities will be available between 0 and 1, which is not desirable in the physical sense of interpretation, hence what is required is a solid-empty scheme where the regions either voids (density = 0) or solids (density = 1). This is achieved by a penalization scheme on the intermediate densities, which is incorporated in the stiffness of every element such that[5]

$$E(x) = \rho(x)^p E^0 \; ; p > 1$$

$$\int_{\Omega} \rho(x)\, d\Omega \leq V; \; 0 \leq \rho(x) \leq 1$$

where $E(x)$ is the young's modulus of an element with density $\rho(x)$, and 'p' is a penalization parameter, which suppresses the intermediate densities, in the sense that if the intermediate densities are included, then the stiffness gained will be much lesser than that with higher densities towards unity – thus making the intermediate densities unfavorable. The second equation expresses the constraint of volume on the problem on the design domain **Ω**.

The stiffness matrix $\boldsymbol{K}$ of the entire structure is the sum of the stiffnesses $\boldsymbol{K_e}$ of every element, which in turn is a function of the Young's Modulus, which has been linked to the design variable (density) as described above. Hence, the formulation is now made as[6]:

$$\min C(\rho, u) = \boldsymbol{U^T K U}$$
$$\frac{V}{V_0} = f$$
$$\boldsymbol{KU} = \boldsymbol{F}$$

Here, $\boldsymbol{U}$ is the global displacement matrix, $\boldsymbol{F}$ is the load vector, and f is the volume fraction of the original volume of the design domain V_0 which has be retained, as a constraint, as discussed earlier.

To avoid singularity in the stiffness matrix $\boldsymbol{K}$, a lower positive non-zero bound is placed on the design variable (density) ρ, such that $0 < \rho_{min} \leq \rho \leq 1$.

The solution is obtained in an iterative process, where, first the initial design is made by homogeneous distribution of material. The entire domain is meshed into finite elements, and the resulting displacements and stiffness are calculated. Then, for each cycle, the design variable is updated (using a gradient based approach, optimality criteria method, etc.) and the calculations are repeated until the compliance obtained in successive cycles converge to a particular value.

2.2 Graphic Statics

2.2.1 Overview of Principles and Methods

Graphic statics is a method perhaps as old as structural engineering itself. Based on the founding works of Maxwell, Cremona and Culmann, it elegantly uses the laws of statics to graphically evaluate the forces in the structural members that are necessary for equilibrium. It follows from the principle of statics that if a set of forces are in equilibrium, their vectors must form a closed polygon.

From the *form diagram* i.e. the representation of the structure, a *force diagram* is constructed. Drawing to a particular scale, the loads are represented by lines parallel to the loads in the form diagram, and the members by similar lines parallel to themselves. Since these are in equilibrium, all these line segments must form a closed polygon.

Bow's notation[7] is most commonly used to identify joints, members, loads and force directions. In the form of the structure, the space between every two load vectors is identified in a clockwise manner by capital letters, and the space in every closed polygon is identified with a numeral. Thus, the members can be identified by reading the letters across them. The force diagram is then drawn by choosing a scale, and plotting every load and reaction by drawing a line segment with length equal to their magnitudes (after converting them from forces to lengths through the scale); the loads and reactions must come to be in balance if the system is in equilibrium. Then, each member is plotted one by one, by making lines parallel to them, and identifying regions through their points of intersection.

For example, the truss shown in Fig 2.8 has spaces between loads and reactions identified as A, B and C, while the space inside the closed polygon of the truss is identified as 1. The form diagram is then drawn by drawing loads as shown on the line *a*-*c*-*b*. To identify member A1, a line parallel to this member from the point *a* on the force diagram is drawn. A similar line is drawn for B1, and point 1 is located as the point of intersection of these lines. Similarly, C1 is plotted too. The lengths of these line segments give the forces in the corresponding members.

To know the direction of the force in a member, a joint to which the member is connected, is chosen. The name of this member is read in the same order in the force diagram, as the order it appears when read clockwise around the joint. This direction, depending on whether it is coming towards the joint or away from the joint, indicates whether it is in compression or tension, respectively.

In the same example in Fig 2.8, to know the direction of force in the member A1, the leftmost node is chosen and going in a clockwise manner, the concerned member is read as A-1. Reading from *a* to *1* in the form diagram, the direction points towards the node, indicating that the member is in compression. In the same way, member B1 is also in compression, while C1 is in tension.

The force diagram is linked to the form in the sense that any manipulation or change in the force diagram brings a corresponding change in the form (and vice-versa). This is very helpful in designing structures, because the designer can directly cater to the geometry of forces and tune them to his purpose to obtain the corresponding form of the structure to fulfill conditions. For examples, arch bridges can be (and have been) designed by this approach[7].

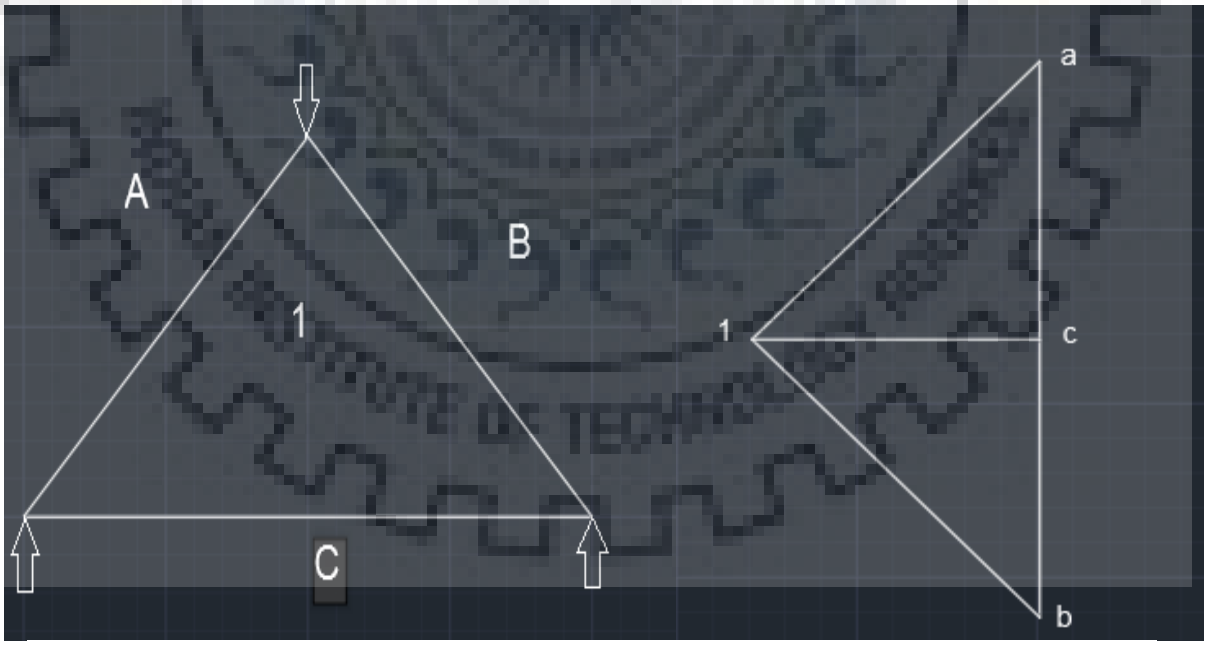

Fig 2.8: *A simple truss used to show the procedure of drawing force diagrams*

2.2.2 Maxwell's Load Path Theorem

Before this theorem is discussed, it will be pertinent to shed some information on the terminology involved in the statement. Assumption is that the structures being dealt with are pin jointed, i.e., they are made up of members carrying only axial forces. If we multiply the length of a member with the magnitude of force carried by it, we get the magnitude of the *load path* for the member. Maxwell's Load Path Theorem says that the difference between the total load path in tension and that in compression is equal to the dot product of all the external forces (with reactions) about any arbitrary point[8]:

$$\sum F_T L_T - \sum F_c L_c = \sum \bar{F} \cdot \bar{r}$$

Here, F_T, F_c are forces in the members in tension and compression, while L_T, L_c are their respective lengths. The right hand side refers to the summation of the dot product of all the external forces $\bar{F}$, the position vector of which from an arbitrary point (same for all the external forces) is $\bar{r}$. This theorem can be directly verified from the Principle of Virtual Work – if a virtual displacement is given by expanding the structure about a point such that all the joints move to positions twice as far as they were originally from that point, then left hand side of the equation refers to the internal virtual work and the right hand side to the external virtual work, hence they both shall be equal[8].

Dividing the load path by the permissible stress σ gives the minimum volume of the member, hence this minimum total volume (for the permissible stress level) can be calculated by

$$V = \frac{1}{\sigma}\sum F_T L_T + \frac{1}{\sigma}\sum F_c L_c$$

Dividing the former by σ and adding it to the latter, we get

$$V = \frac{1}{\sigma}(2\sum F_T L_T - \sum \bar{F} \cdot \bar{r})$$

Maxwell's Load Path Theorem can thus be directly used to determine the minimum volume of a structure for a given stress level by computing only the external force dot product and the tensile (or compressive) load path, depending upon the convenience of the designer.

CHAPTER 3 – OBJECTIVES

Following are the objectives of this study:

1. To investigate the outcome of optimum bridge forms for a uniformly distributed load condition, from a Minimum Compliance with Weight Constraint (MCWC) approach, and compare the results with those obtained from Minimum Weight with Stress Constraint (MWSC) approaches.

2. To investigate the forms of arch bridges obtained under compliance minimization with a constraint over the total volume available for the final form, and to observe the effects under different rise to span ratios.

3. To investigate the bridge forms obtained under the same objective and constraint, over a continuous domain with boundary conditions analogous to that of bridges with long spans, and to validate the results with those obtained by applying a weight minimization objective over a discrete domain.

4. To study the obtained bridge forms using Graphic Statics to get an insight into their behavior and peculiarities.

CHAPTER 4 – METHODOLOGY

In this study, a *continuous design domain* is used, which is provided with boundary conditions similar to those in bridges. A uniformly distributed load is applied on the structure to simulate the dead load. Live loads, which may also be asymmetric, are not included, because the dead loads which are always present have a more decisive effect on the overall form of the structure; and in addition, live loads are insignificant compared to dead load especially in long span bridges. The objective of the optimization is to minimize the strain energy of the structure, when a constraint over the volume available for the final structure is placed on it. The SIMP approach is adopted for the optimization process.

4.1 Optimization of Arch Forms on *Tosca/Abaqus 2019*

A study of the optimization of arch forms is made on the structural optimization module *Tosca* that comes in conjunction with *Abaqus 2019* software package.

Arch bridges conventionally are used for low to medium spans. Keeping that in mind, a rectangular design domain (Fig 4.1) 50 m in length is chosen. The height of this domain is varied in accordance to rise to span ratios ranging from 0.1 to 1, in equal intervals of 0.1. The design domain is considered to be in plane stress with a thickness of 0.2 m. A uniformly distributed load of 40 kN/m is applied to the bottom of the design domain. One of the ends is kept hinged, while the other is kept on roller supports. 4-Noded Bilinear elements are used with mesh size = 0.25 m.

Steel with $E = 2 \times 10^5\ MPa$, density = 7850 kg/m^3 and poisson's ratio = 0.3 is used as material. Plasticity is not taken into account because strain energy ceases to be a relevant parameter once plastic flow begins – energy dissipation begins to occur and external work is no longer converted into strain energy.

In the optimization module, strain energy is set to be the objective function, and constraint is set on the final desired volume of the structure by setting a *volume fraction* which is the ratio of the desired final volume to the original volume of the design domain. In the process of optimization, the minimum value of design variable (which is the normalized density of an element) is taken as 0.001 and the penalization power is taken to be 3, for the validity of the model as material behavior.

For each rise to span ratio (from 0.1 to 1), the volume fraction is ranged from 0.1 to 0.5 in intervals of 0.1. Thus, a total of 50 models are prepared, and the resulting optimized arch forms from each are obtained and studied further.

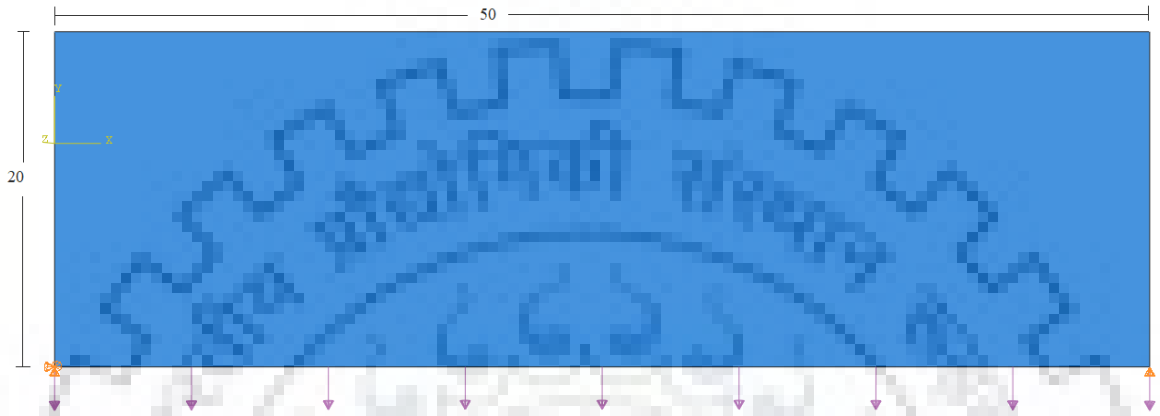

Fig 4.1: *Design domain with dimensions (mm), loading type and boundary conditions. Model corresponds to a rise : span of 0.4.*

4.2 Optimization for Long Span Bridge Forms in *Tosca/Abaqus 2019*

Long span bridges have, typically, a main, longer central span(s) and smaller side spans. For reasons of symmetry and intuition from literature survey about Michell's ideal forms, the model is made with a central span of 3 km and two side spans of lengths equal to half the main span, i.e. 1.5 km each. This is similar to problem of finding the optimum (weight) structure to support a horizontal beam running infinitely, supported over equally spaced pin joints. However, in this case the objective is to minimize the strain energy of the system.

A rectangular design domain (Fig 4.2) 6 km in length is chosen, with two pin supports spaced symmetrically at 1.5 km from either ends, such that a central main span of 3 km and two side spans of 1.5 km are achieved. The design domain is given horizontal supports at the both the bottom ends - this is because the model will be a perfect idealization of the infinite horizontal problem as the loads will be supported throughout by the superstructure alone; and moreover, the end anchorages give approximately a horizontal reaction only for many bridges, including the Akashi Kaikyo Bridge[4]. The height of the design domain is kept to be 1600 m, to let any resulting optimum form develop fully, unrestricted by height of domain. The design domain is

considered to be in plane stress with a thickness of 1m. A uniformly distributed load of 400 kN/m is applied on the bottom of the design domain. 4-noded bilinear quadrilateral elements are used. Initially, a mesh size of 1 m is used.

The material of the model and optimization objective are same as in the previous case of arch bridge forms. A volume fraction of 0.13, deliberately kept low for better visualization of results, is selected after some trials and observations.

Since the span is very long, a non-linear analysis is also done and results are compared with those of linear analysis made under similar conditions. The results of the bridge forms obtained are studied further.

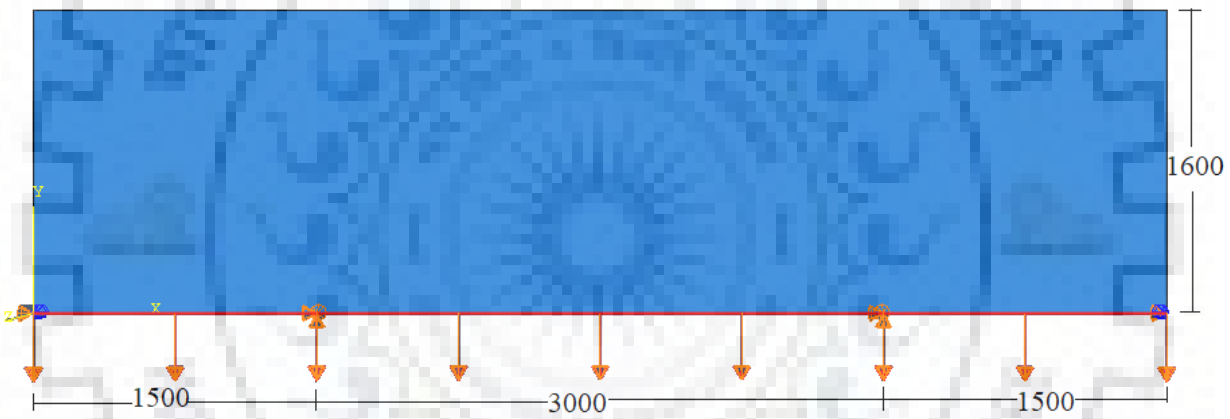

Fig 4.2: *Design space for long span bridge with dimensions (m), loading type and boundary conditions.*

4.3 Changing Limiting Compressive to Tensile Stress Ratio in *Rhino 3D*

Unsurprisingly, the optimization process in Tosca is not suitable for constraints on stress because of the numerous difficulties that occur in topology optimization using stress constraints. This is because the concerned optimum points often lie in a degenerate subset of the feasible region which cannot always be located by gradient-based optimization algorithms. In addition to it, the number of variables is as same as the number of responses because stress is a response at a local point or element and is hence defined for every element, while responses like volume and strain

energy are global, hence computationally much more feasible to be dealt with in topology optimization.

Grasshopper is a visual programming environment that runs on *Rhinoceros 3D* - a computer aided design software which allows to create models. A circuital flowchart type methodology is followed by Grasshopper, where items are assigned to entities which are then assembled on the canvas as per logic of the operation. An experimental topology optimization plugin, TopOpt, runs in grasshopper that allows the user to change the ratio of allowable compressive to tensile stresses. However, the outputs obtained for large dimensions of design space are unremarkable in visual clarity due to the limitations of filter size. Noting that topology optimization is dependent on the loading type, boundary conditions and geometric similarity of the design domain (and not on any magnitudes of these), a small-scale model emulating the same kind of long span bridges as discussed earlier, is made.

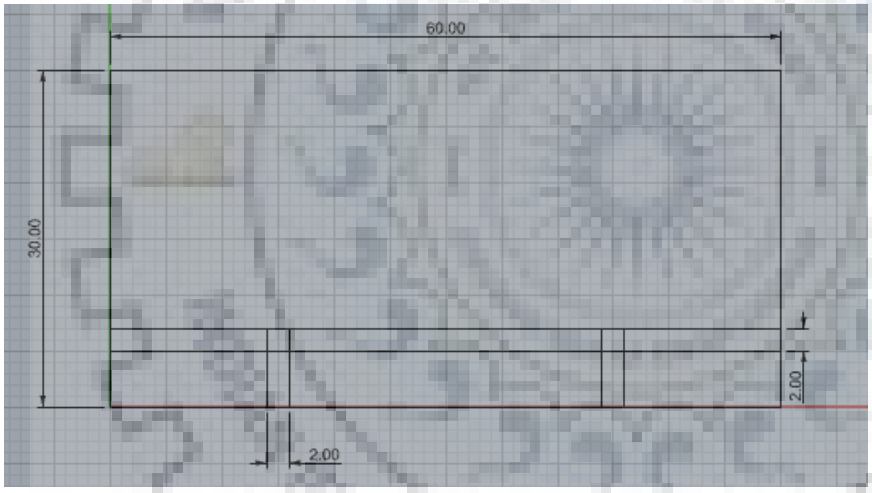

Fig 4.3: *Dimensions of the design space in Rhino 3D. The 2 mm thick rectangles are frozen as solids, and the adjoining ones as voids.*

The design domain (Fig 4.3) is taken to be a rectangle, 60 mm in length, 30 mm in height and 1 mm in thickness (for plane stress conditions). The value of Young's Modulus is taken to be 1, and the mesh size as 1 mm without a loss of generality, as the effect is only to have the numerical results scaled without any effect on the topology. It is supported symmetrically by two pin line supports of 2mm each at quarter and three-quarters length, with regions frozen as voids and solids as shown in Fig 4.3. The layout of the visual flowchart of operations as made in *Grasshopper* is shown in Fig 4.4.

The volume fraction is kept at 0.15 for obtaining the best clarity of form, and the filter radius is set at 1.5 – below that, the output displays checkerboard solutions, and greater filter radii tend to give solutions with 'smeared' densities. The parameter *ratio*, which signifies the ratio of

allowable compressive to tensile stress, is changed and the resulting optimized bridge form obtained for every chosen instance of *ratio* is noted.

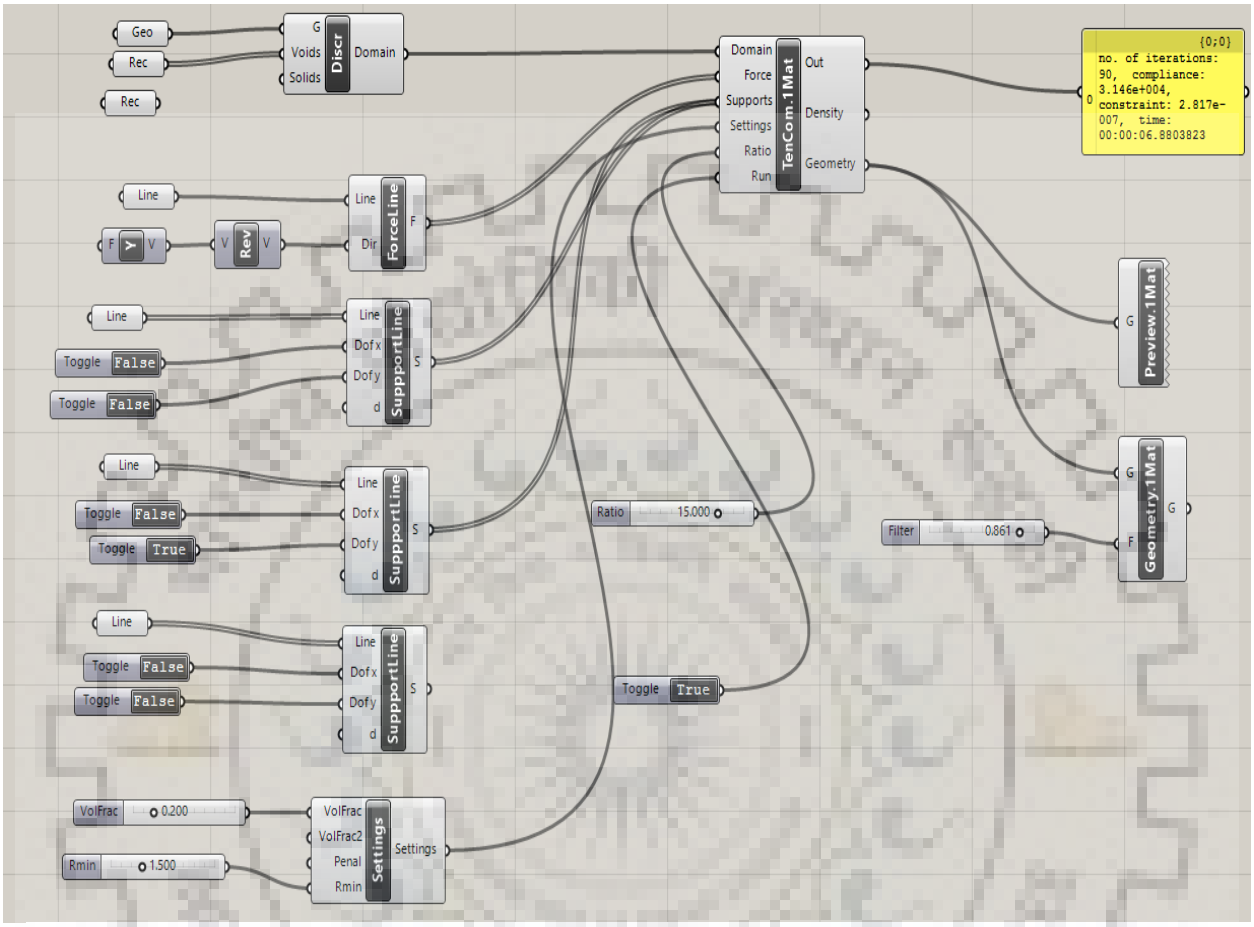

Fig 4.4: *Grasshopper canvas with parameters assigned to components that are arranged in a circuital flow chart.*

4.4 Interpretation using Graphic Statics

Principles of Graphic Statics, like the relationship between the form and force diagram, peculiarities in the force diagram when the structure is biased towards a certain behavior, and Maxwell's Load Path Theorem are used to analyze and interpret the various bridge forms that are obtained as a result of the optimization process.

CHAPTER 5 – RESULTS AND INTERPRETATION

5.1 Optimization of Arch Forms on *Tosca/Abaqus 2019*

5.1.1 Bridge Forms Obtained: Observations

As described in the previous section, optimization for minimum strain energy is performed over the defined design domain with volume constraints formulated as volume fractions. To volume fractions (denoted by *vfrac* in the following figures and tables) are chosen as 0.1, 0.2, 0.3, 0.4 and 0.5 for every rise to span ratios in the geometry, which are chosen ten in number, starting from 0.1 till 1.0.

The strain energy at the end of every optimization procedure is noted which is presented in Fig 5.1. The horizontal axis has the rise to span ratios, while the vertical axis has strain energy of the optimized structure. Table *A-1* has been used to construct the graph which is provided in *Annexure – A.*

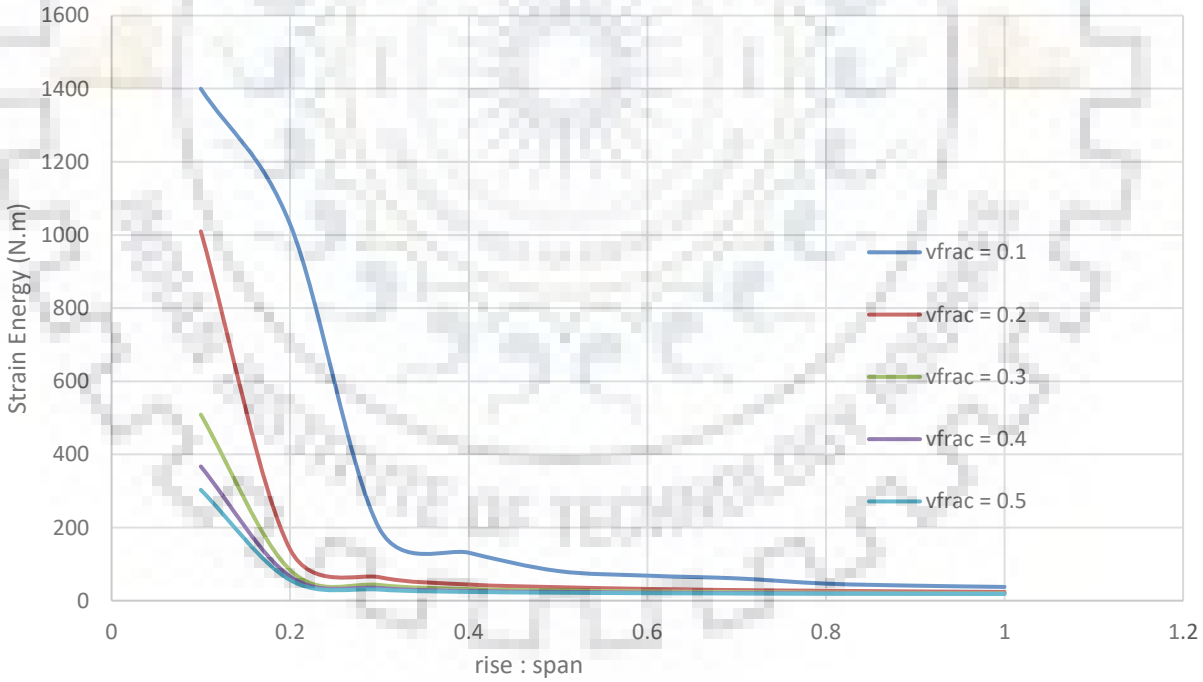

Fig 5.1: Effect on strain energy by changing rise to span ratios for various volume fractions.

Following observations can be made from the graph and obtained output of the forms:

- For small volume fractions, strain energies of the optimized arches are comparatively very high when rise to span ratio is small.

  This is because on one hand, the small rise to span ratio restricts the arch action from developing fully, and on the other, the small amount of available volume is not sufficient for attaining other forms (like that of a truss). Hence, a shallow, flat arch is generated which has low stiffness and hence high strain energy.

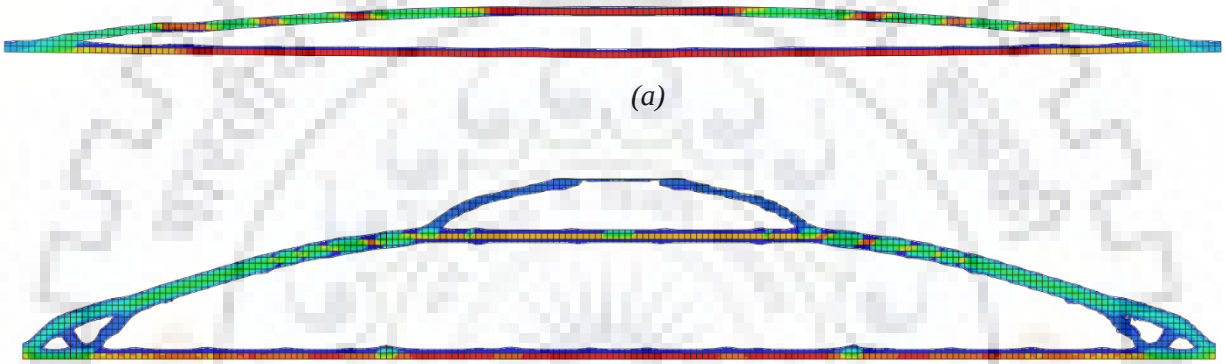

(a)

(b)

Fig 5.2: *Two forms, corresponding to volume fraction of 0.1 for a rise : span of (a) 0.1; (b) 0.2*

The form shown in Fig 5.2-*(a)* has a strain energy of 1400 N.m, while the one in Fig 5.2-*(b)* has a strain energy of 1010 N.m. In the latter, the structure is shown changing its form from an arch type to a truss type.

- If the rise to span ratio is less than 0.2 – 0.25, then for a particular value of this ratio, increasing the volume fraction rapidly decreases the strain energy. It means that for shallow domains, adding more volume rapidly increases the stiffness of the structure. For example, in Fig 5.3, *(a)*, *(b)* and *(c)* have strain energies of 1400 N.m, 508.7 N.m and 303 N.m, respectively. The huge drop in strain energies from *(a)* to *(b)* can be attributed to change in form from that of a shallow arch to a truss.

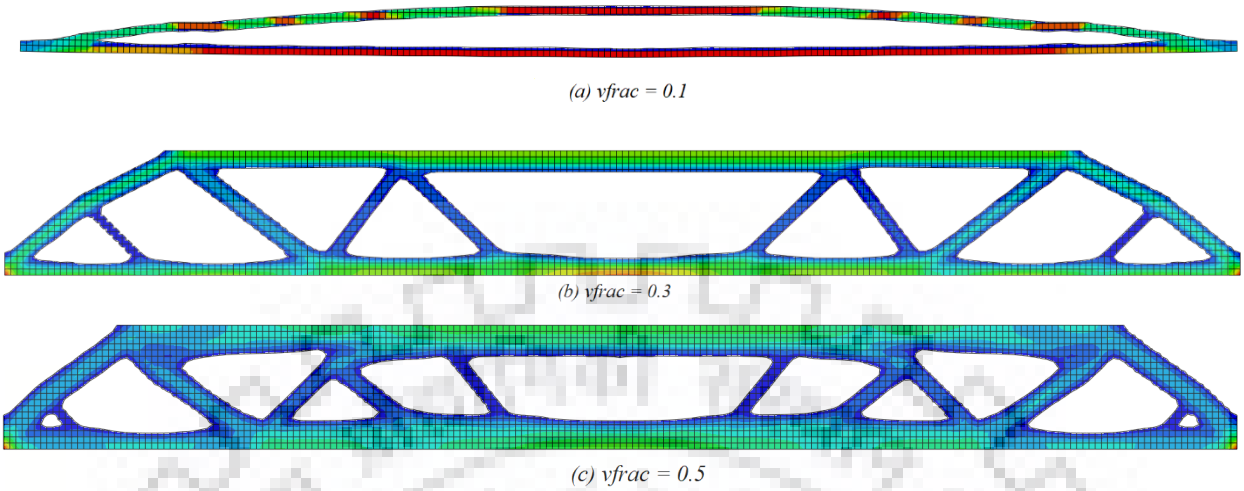

Fig 5.3: *Three forms, corresponding to rise : span of 0.1, for volume fraction (a) 0.1; (b) 0.3; (c) 0.5. These forms have highest strain energies for their respective volume fractions.*

- After the rise to span ratio has crossed that range, then for a particular value of this ratio, increasing the volume fraction has very low effect on decreasing the strain energy. It means that once a sufficient depth of the domain has been reached, adding more material adds little to the improvement in the stiffness of the structure. The form is already found and the extra material is just deposited over this form (Fig 5.5 – 5.7).

- If the volume of the final structure is kept constant and it is allowed to be distributed for different rise to span ratios, it is found that the structure formed goes from truss form to arch form once the rise to span ratio of 0.2 – 0.25 is crossed. The strain energy falls rapidly with rise to span ratio (till 0.2-0.25), and then the drop is negligible (Fig 5.4, Fig 5.8 – 5.10).

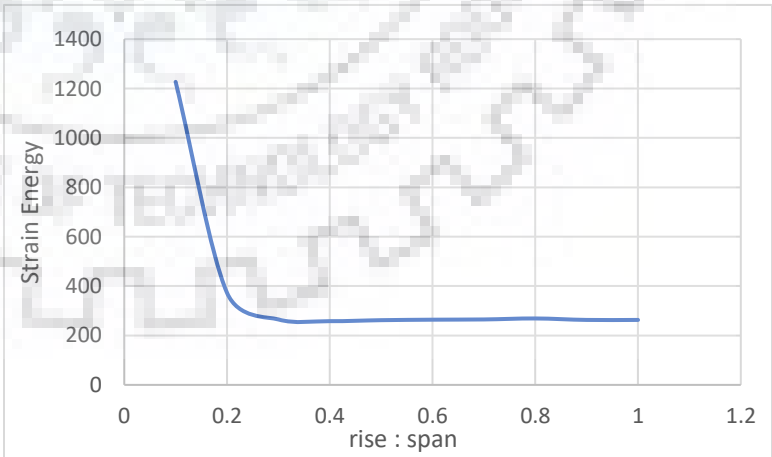

Fig 5.4: *Variation of strain energy with rise : span for a constant volume (35 m^3). Refer Table A-2 in Annexure – A.*

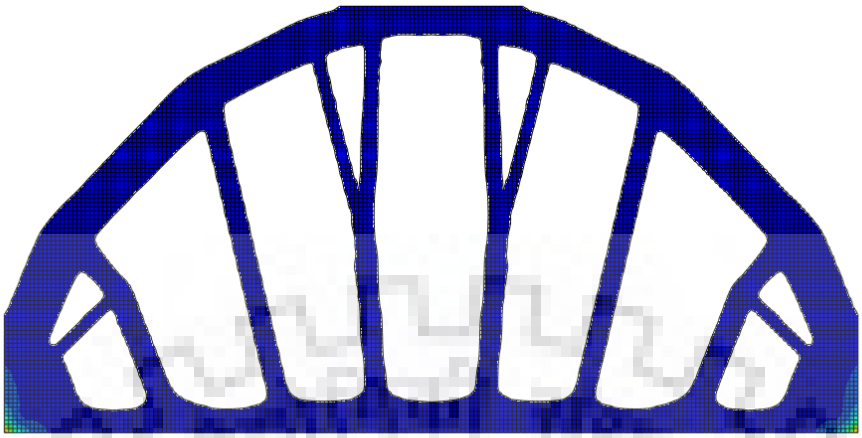

(a)

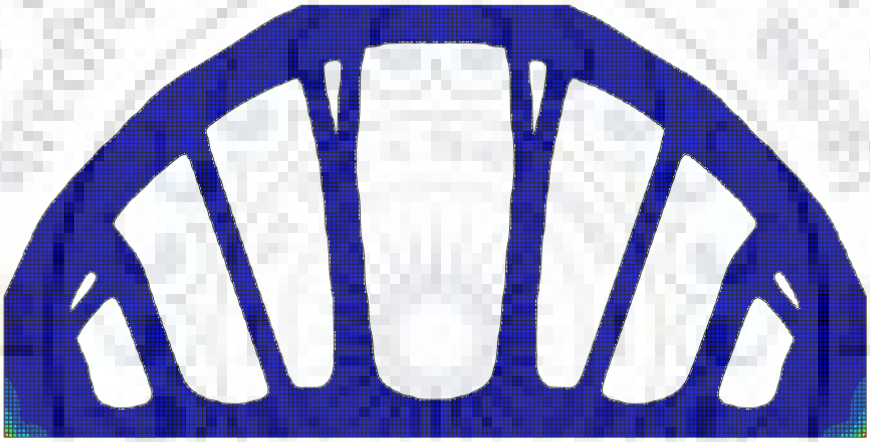

(b)

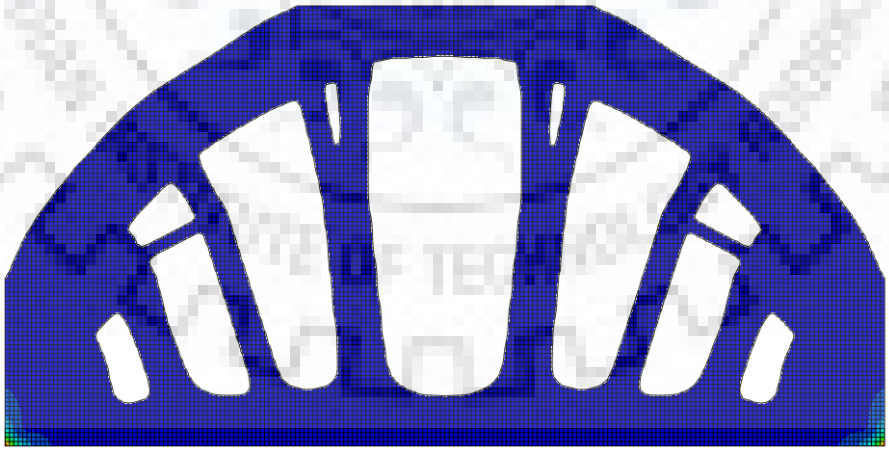

(c)

Fig 5.5: Forms obtained for a rise : span ratio of 0.5 for volume fractions (a) 0.3; (b) 0.4; (c) 0.5.

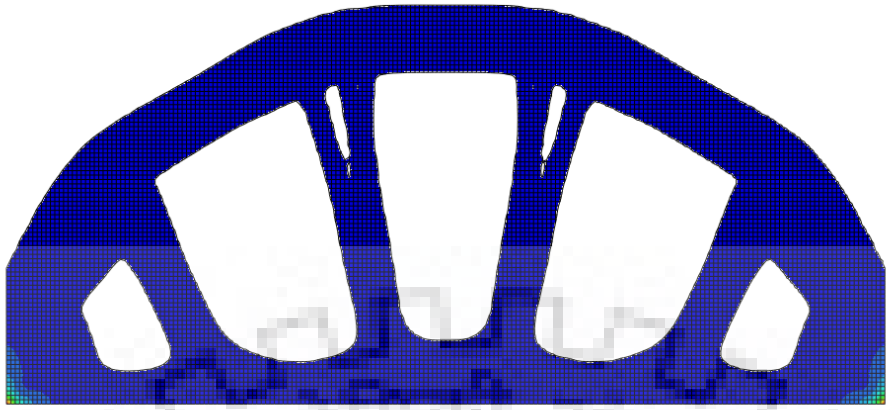

(a)

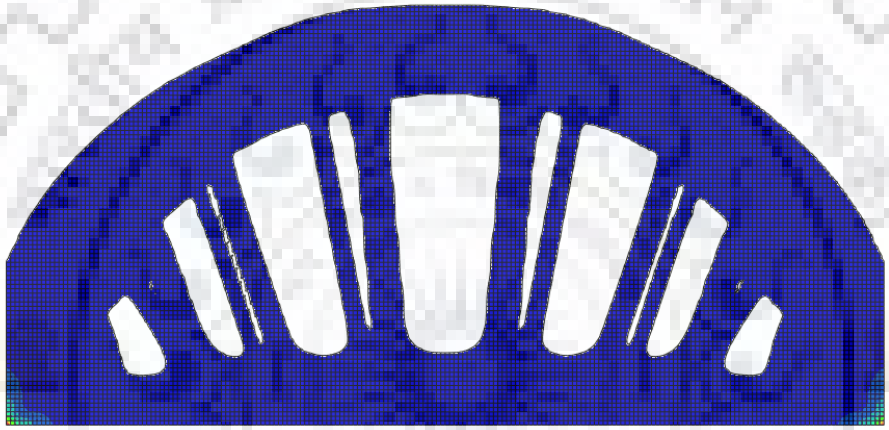

(b)

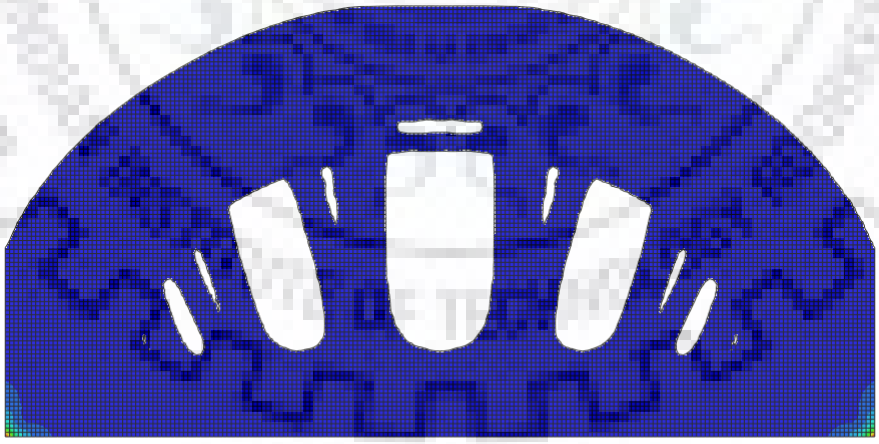

(c)

Fig 5.6*: Forms obtained for a rise : span ratio of 0.7 for volume fractions (a) 0.3; (b) 0.4; (c) 0.5.*

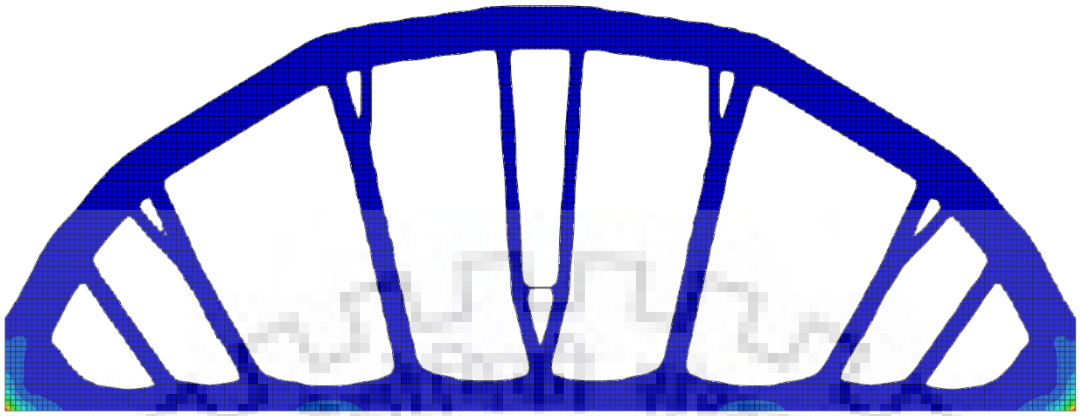

(a)

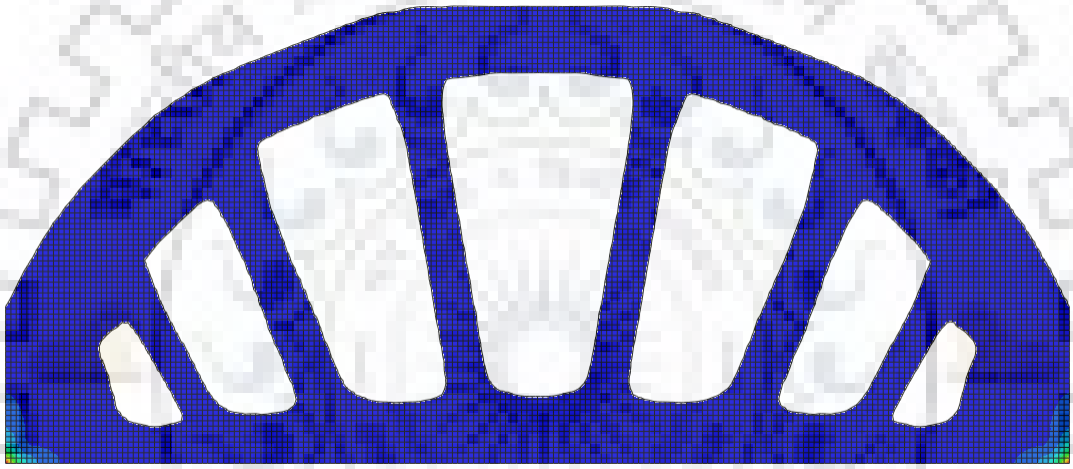

(b)

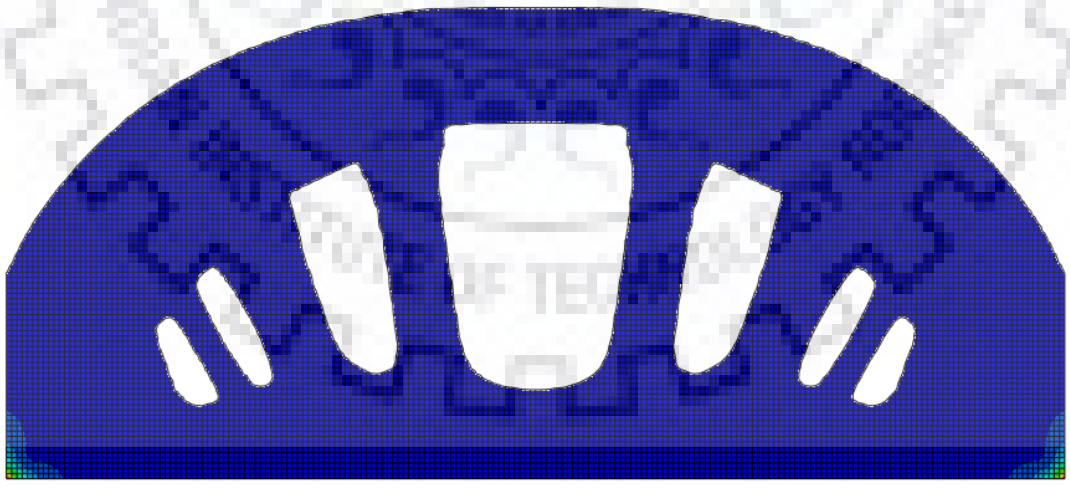

(c)

Fig 5.7*: Forms obtained for a rise : span ratio of 1 for volume fractions (a) 0.1; (b) 0.2; (c) 0.3.*

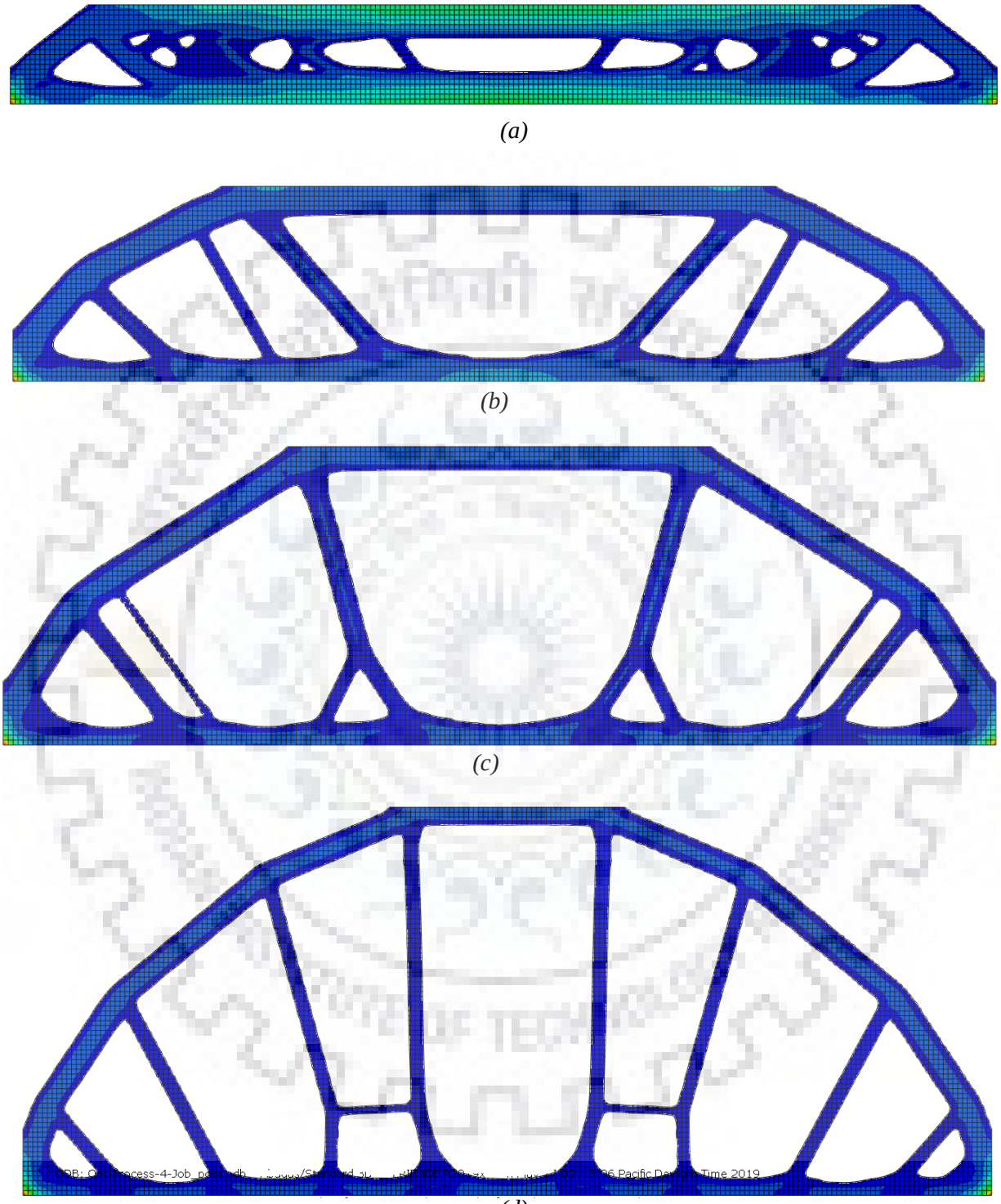

(a)

(b)

(c)

(d)

Fig 5.8*: Forms obtained for a rise : span ratio of (a) 0.1; (b) 0.2; (c) 0.3; (d) 0.4 for a constant volume (35m^3)*

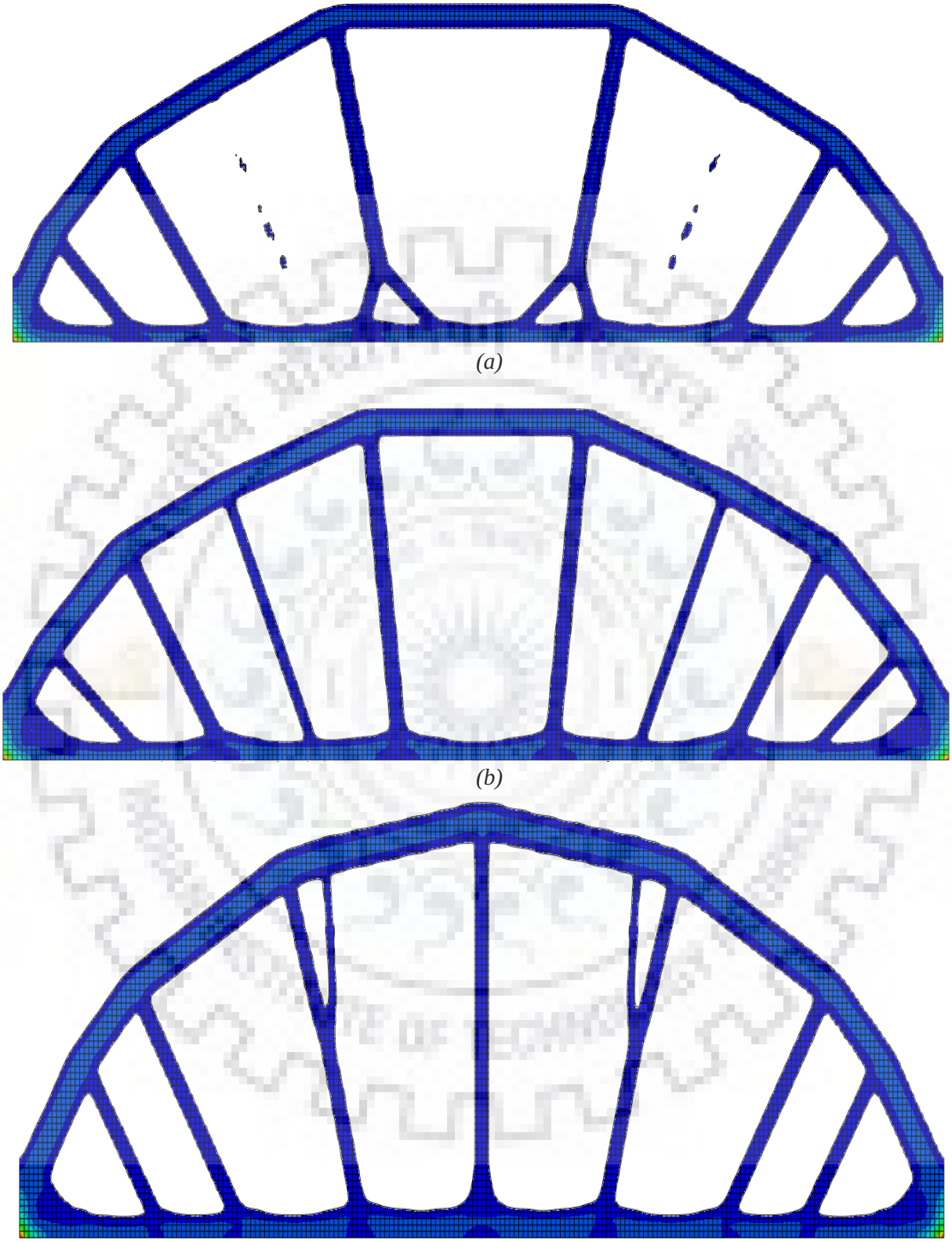

(a)

(b)

(c)

Fig 5.9*: Forms obtained for a rise : span ratio of (a) 0.5; (b) 0.6; (c) 0.7 for a constant volume (35 m^3)*

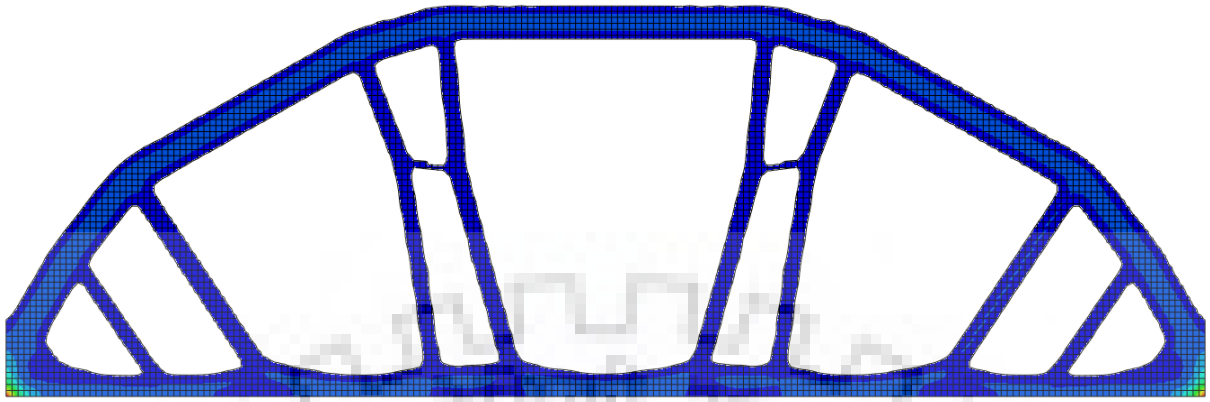

(a)

(b)

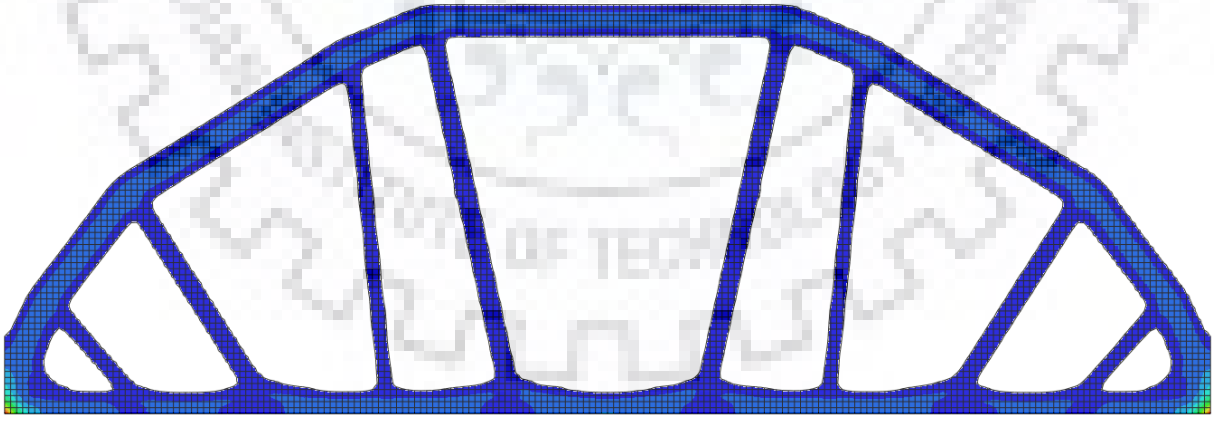

(c)

Fig 5.10*: Forms obtained for a rise : span ratio of (a) 0.8; (b) 0.9; (c) 1.0 for a constant volume (35 m^3)*

5.1.2 Interpretation of Results

All the arch forms obtained have a common characteristic – they are uniformly stressed in the arch rib which remains constant in depth in every form obtained, while the hangers are having negligible stress compared to the arch ribs. Thus, the design obtained corresponds to the design for an arch (bowstring) bridge with constant force in the arch segments, and the load transfer takes chiefly through the arch. The form and force diagram are shown below in Fig 5.11.

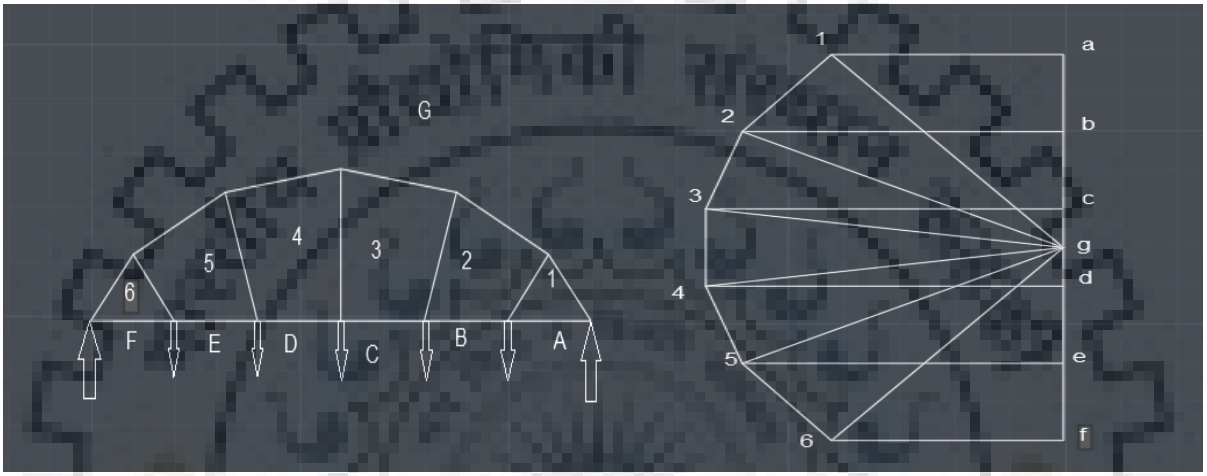

Fig 5.11: *Form and force diagram for an arch bridge with constant force in the arch segments.*

Increasing volume fraction has very low effect on diminishing the strain energy, once a particular range of rise to span ratio is crossed. This can be interpreted in the following manner. For very shallow bridge heights, the *arch action* is not developed fully, so while an arch is formed for very low volume fraction (0.1), it is not the most efficient in stiffness. Hence, when more volume is supplied to such shallow heighted domains, it gets redistributed to form the *truss* type form with the top member running along the top of the domain, and the stiffness increases, decreasing the strain energy.

As the height of the domain is increased, the arch action develops further till it is completely developed around the rise to span ratio of 0.2 – 0.25. Thereafter, the supplying more volume doesn't result in any better arch action, hence the improvement in stiffness is unremarkable. Further supplied volume is simply deposited on the already acquired form, making the members thicker and diminishing the stresses.

When a constant volume is distributed across domains with different rise to span ratios, the material is forced into a truss form when the depth is shallow, and as the depth increases it assumes the form of an arch with constant force. The hangers are negligibly stressed, and the load is chiefly carried through the arch and tie action.

The magnitude of load has little effect on the form of an arch bridge which carries constant force in it's arch segments. It can be demonstrated through form and force diagram shown in Fig 5.12. In this figure, the loads acting on the arch bridge shown in Fig 5.11 have been doubled. It is shown that the orientation of the members remains the same, only that the forces in them get magnified. It can be noted from the force diagram that the hangers are carrying quite less forces as compared to the arch segments, which explains them being low in stresses as obtained in the results.

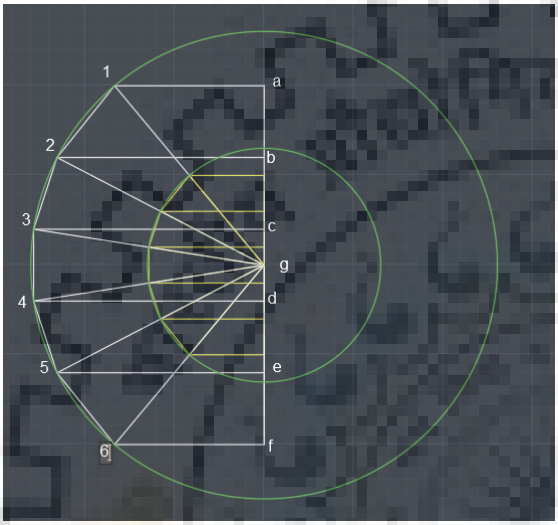

Fig 5.12: *Force diagram for constant force in the arch segments when loading is doubled; concentric circles are arch force envelops.*

5.2 Optimization of Long Span Bridge Forms on *Tosca/Abaqus 2019*

The details of the model have been provided in Chapter -4. Objective function remains to minimize the strain energy of the structure.

For a volume fraction of 0.13 (chosen to get the best clarity in form) and mesh size of 1 m, the following bridge form is obtained (Fig 5.13).

Fig 5.13: *Bridge form obtained for volume fraction of 0.13.*

The strain energy for this structure is 1.72×10^8 N.m, and the central deflection is 1.42 m.

When the mesh size is changed to 5m, the strain energy of the structure is obtained as 2.24×10^8 N.m and the central deflection is 1.04 m. Since the deflections are large, geometric non-linearity is incorporated in analysis and the resulting form has a strain energy of 2.17×10^8 N.m, deflecting 2.38 m at center. Bridge form obtained is the same in both the cases, shown in Fig 5.14.

Fig 5.14: *Bridge form obtained for volume fraction of 0.13 with a mesh size of 5 m. Same form is obtained for a non-linear analysis.*

These bridge forms can be seen to have two kinds of optimal regions, an inner region in which tensile and compressive members cross orthogonally, and an outer region that contains only tensile members.

These forms match with those obtained by Pichugin et al. in <Fig> and Gilbert et al in <Fig> which they have obtained by optimizing a discrete design domain under stress constraints. Thus, it can be seen that forms optimum for least weight under stress constraints are also optimum for maximum stiffness, or minimum strain energy for particular volume constraints. In a way, the validity of SIMP as a material model is also established, because it replicates the results that are obtained by the ground structure approach.

5.3 Changing Limiting Compressive to Tensile Stress Ratio in *Rhino 3D*

The ratio of limiting compressive to tensile stress is changed and optimization is performed for minimum strain energy keeping the constraint of volume fraction fixed to be 0.15. This value of volume fraction is chosen so that the best resolution for the visual output can be obtained. If the mentioned ratio is greater than unity, then the design is compression dominant; on the other hand, keeping the ratio less than unity makes the design dominant towards tension.

Following is the variation of the strain energy with varying ratios of limiting compressive to tensile stress (mentioned in the graph as *ratio*). Table *A-3* for the data sets can be found in Annexure A.

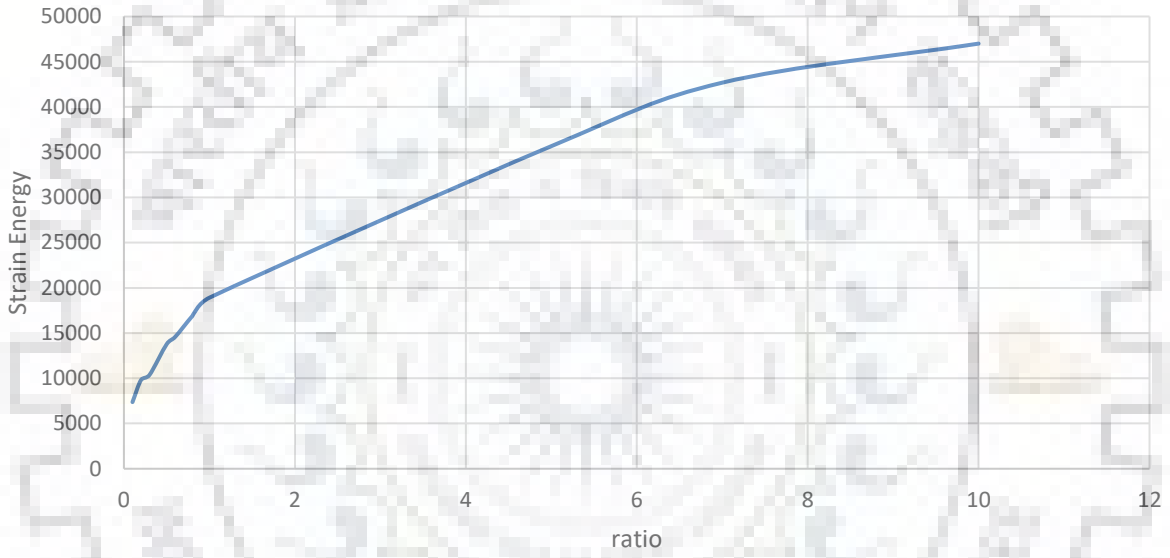

Fig 5.15: *Variation of strain energy with the limiting tensile to compressive stress ratio*

It is observed that the strain energy keeps monotonically decreasing as the design is made dominant towards tension by decreasing the *ratio*. Tension dominant structures, for the same amount of volume, are stiffer than compression dominant structures when optimized for minimum strain energy. Prima-facie, this appears to be an anomaly.

On the following page, the shapes revealed for some typical *ratios* are depicted in Fig 5.16, and they are validated with the forms available in the literature obtained through weight minimization with stress constraints, using the discrete *ground structure* approach.

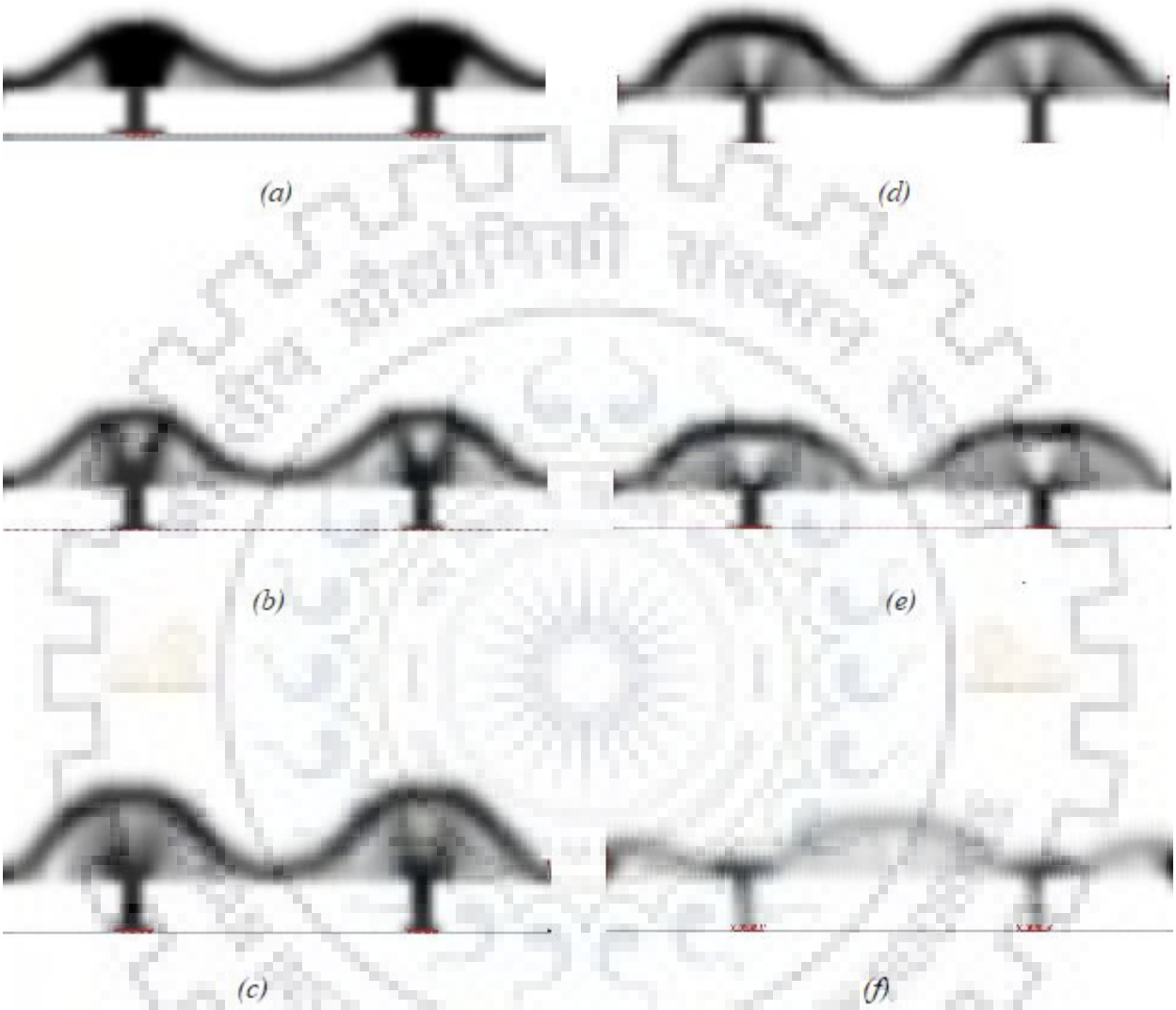

Fig 5.16: *Bridge forms obtained for volume fraction = 0.15, and ratio (a) 0.1; (b) 0.5; (c) 1.0; (d) 5; (e) 8; (f)10*

It can be observed that as the *ratio* is decreased below 1, the spokes of the wheel shrink together to form pylon-like structures and come closer as the ratio is further decreased, to resemble cable stayed forms. When the *ratio* is increased above ten, the structure degenerates into arch forms with spurs radiating from supports to the arch rib, and when the *ratio* is sufficiently high, it forms an arch with vertical suspenders. This is in consistence with the findings of Pichugin et al. who employed weight minimization on a discrete ground structure with stress constraints.

A suspension bridge can also be obtained as an optimum form by changing the boundary conditions – pinned line supports provided at the top of the design domain, exactly at the ordinate and of the same length as the intermediate pinned line supports, simulate the presence of a upwards prop <Fig>.

However, the strain energy of the resulting suspension form (Fig 5.17) is much greater than the Mitchell's form. For example, for a volume fraction of 0.3, Michell's form comes to have a strain energy of 8.71×10^3 while the suspension form has a strain energy of 4.053×10^7 N.m.

Fig 5.17: *Suspension bridge form obtained for volume fraction = 0.30, by changing the boundary conditions on the design domain*

Fig 5.18: *Checkerboard pattern observed in the form output for filter radius = 1*

This was the best resolution that could be obtained with the filter radius of 1.5 recommended in the SIMP procedure. Using a lower filter than this gives checkerboard problem where there are alternate stiff and soft regions giving a spurious stiffness (Fig 5.18), and using a higher filter radius gives a 'smeared' output difficult to visually interpret.

Fig 5.19: *Form for ratio = 0.13 by Baker et al. (2015)*

The form obtained for *ratio* of 0.13 for weight minimization using stress constraints by Baker et al[8]. is shown in Fig 5.19. It can be readily seen to be similar to the form obtained by the present analysis, shown in Fig 5.16 *(a).*

CHAPTER 6– DISCUSSION

❖ *On the width of optimal region – T in Michell's hybrid structure*

As was observed, Michell's hybrid structure consists of two kinds of optimal regions, R^+ and T, marked by a vertical transition line. Members in the R^+ region are straight and they shoot off as tangents to the arcs in the T region.

The width of the T region can be calculated using Maxwell's Theorem. Let the span be of length *2L*. A single element of the hybrid structure is considered of radius *r*, with it's transition defined by the point (x_r , y_r). Distance of the point where this member meets the horizontal at angle α is denoted by L_r. The loads at the ends of the members is *F* and hence the total vertical reaction is *2F* at *O* (Fig 6.1)

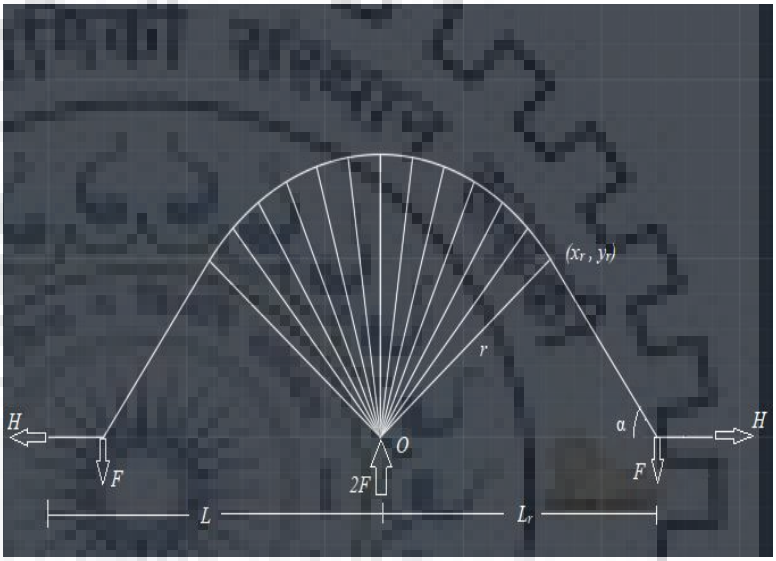

Fig 6.1: *Geometry and loading on an element taken from the Michell's hybrid structure*

The circular arc at the top, the tangential member and the horizontal link are in tension. They are summarized as below.

Member	Length (L_T)	Force (F_T)	$L_T \times F_T$
Arc (1 in number)	$2\alpha r = 2\alpha L_r \sin\alpha$	$\frac{F}{\sin\alpha}$	$2F\alpha L_r$
Tangent (2 in number)	$L_r \cos\alpha$	$\frac{F}{\sin\alpha}$	$\frac{FL_r}{\tan\alpha}$
Link (2 in number)	$L - L_r$	$\frac{F}{\tan\alpha}$	$\frac{F\,(L - L_r)}{\tan\alpha}$

Table 6.1: *Lengths and forces of tension members in the element*

Dot Product of forces $\sum \bar{F} \cdot \bar{r}$ can be found by choosing the origin *O* as the reference point. Only the horizontal pull *H* has a non zero dot product. This comes out to be

$$\sum \bar{F} \cdot \bar{r} = \frac{2FL}{\tan \alpha}$$

For allowable stress σ, total volume, thus by Maxwell's Law is given by

$$\frac{1}{\sigma}(2\sum F_T L_T - \sum \bar{F} \cdot \bar{r}\,) = \frac{2}{\sigma}\left(2F\alpha L_r + \frac{FL}{\tan \alpha}\right)$$

Differentiating with respect to α, we get

$$L_r = \frac{L\, cosec^2 \alpha}{2}$$

Noting that $x_r = L_r sin^2 \alpha$, we get

$$x_r = \frac{L}{2}$$

In other words, the *T* region has a width half of the span. As given by Pichugin et. al, this distance is given by[3]

$$L_r = \frac{\sigma_c L}{\sigma_c + \sigma_T}$$

When the permissible stress is same both in tension and compression, the same result is obtained as through Maxwell's law.

CHAPTER 7– SUMMARY AND CONCLUSIONS

Following have been the salient observations made in this study:

- Structures optimized for weight under stress constraints are similar to those optimized for compliance (or strain energy) under volume constraints, if the material is in elastic range. This is corroborated by the validation of the forms for long spans obtained in this study through compliance minimization, with the forms optimum for weight under stress constraints presented in literature.

- Arch forms are more efficient in stiffness than truss forms for same volume of material used. For arch action to be fully developed, a certain amount of depth has to be available, or the material is constrained to form into a truss system. A rise to span ratio of 0.2 – 0.25 appears to be the value around which it develops fully.

- Optimum arch bridges use arch and tie action for load transfer. The arch (and tie) are under constant force (stress) while the suspenders carry relatively little load.

- For sufficiently deep arches, adding material makes insignificant changes to the stiffness and the optimum form.

- Hybrid Michell form is best suited for the configuration of long span bridges, although it may be difficult to construct owing to complex geometry.

- Changing the ratio of allowable compressive to tensile stresses gives a family of bridge forms even for compliance minimization under volume constraints. At the end of compression dominance lie arch forms, while cable stayed forms lie at the end of tension dominance. However, the tension dominant forms show to be stiffer than the compression dominant forms.

REFERENCES

1. Hemp, W.S. (1974), Michell framework for uniform load between fixed supports, Eng Optim 1:61-69.
2. Rozvany, G.I.N., Bendsøe, M.P., Kirsch, U. (1995), Layout optimization of structures, American Society of Mechanical Engineers.
3. Pichugin, A.V., Tyas, A., Gilbert, M., & He, L. (2015), Optimum structure for a uniform load over multiple spans, Springer-Verlag Heidelberg.
4. Fairclough, H. E., Gilbert, M., Pichugin, A. V., Tyas, Andy, Firth, Ian (2018), Theoretically optimal forms for very long-span bridges under gravity loading, The Royal Society Publishing.
5. Bendsøe, M. P., Sigmund, O. (2003), Topology optimization: theory, methods and applications, Springer, Berlin.
6. Sigmund, O. (2001), A 99 line topology optimization code written in Matlab, Springer-Verlag.
7. Allen, E., Zalewski, W. (2010), Forms and Forces, John Wiley & Sons, Inc.
8. Baker, W. F., Structural innovation: combining classic theories with new technologies.

ANNEXURE - A

rise : span	Strain Energy (N.m)				
	vfrac = 0.1	vfrac =0.2	vfrac =0.3	vfrac =0.4	vfrac = 0.5
0.1	1400	1010	508.7	367	303
0.2	1029	140	83.7	66.3	56.4
0.3	196.8	64.1	42.8	34.7	30.3
0.4	131.1	44.1	31.9	26.7	23.9
0.5	81.1	36.8	28	24	21.7
0.6	68.4	32.1	25.2	22.1	20.4
0.7	60.9	28.9	23.3	20.8	19.6
0.8	46.6	27	22.1	20	19
0.9	41	25.2	21.2	19.5	18.7
1.0	37.5	23.9	20.5	19.2	18.3

Table A-1: *Data points for Fig 5.1*

rise : span	Strain Energy (N.m)
0.1	1227
0.2	373
0.3	265
0.4	258
0.5	262
0.6	264
0.7	265
0.8	269
0.9	263
1.0	263

Table A-2: *Data points for Fig 5.4; volume taken is 35 m^3.*

Ratio	Strain Energy (units)
0.1	7367
0.2	9810
0.3	10380
0.5	13770
0.6	14580
0.8	16880
1.0	18910
5.0	35660
7.0	42680
10.0	47000

Table A-3: *Data points for Fig 5.15*